UNIVERSIDADE DE LISBOA
FACULDADE DE CIÊNCIAS
DEPARTAMENTO DE QUÍMICA E BIOQUÍMICA

C-glycoside synthesis towards innovation in antimicrobials

Patrícia Ferreira Calado

Mestrado em Química
Especialização em Química, Saúde e Nutrição

Dissertação orientada por:
Professora Doutora Amélia Pilar Rauter

2019

Acknowledgments

First of all, I would like to thank my dissertation supervisor Prof. Drª Amélia Pilar Rauter for teaching me organic chemistry since my graduation's first year, encouraging me to pursuit my desire to study the carbohydrates, providing me with the necessary scientific guidance and support and also enthusiasm. I want to thank the opportunities I had, namely the summer research in Beijing University of Chemical Technology (BUCT) which was a truly enriching cultural experience.

I would like to express my deep gratitude to Drª María Teresa Blázquez Sánchez for constantly being available to help me solving the emerging problems, giving me the best advices and guiding me throughout this past year. I appreciate a lot the love and support that she always gave me. I also want to thank Prof. Drª Maria José Brito for helping me with NMR experiments and compounds' characterization, and Prof. Drª Suying Xu for helping me to adapt to the Chinese culture as well as integrating me in her research group. To João Pedro Pais, I want to thank the help given when I was writing my dissertation.

To my colleagues and friends from the Carbohydrate Chemistry group, Andreia Fortuna, Ana Baptista, Bernardo Henriques, Eduardo de Sousa and Vítor Martins, thank you for the friendship, conversations and emotional support. Also, to Rafael, Tiago Gomes, Catarina Cipriano, Lucas Prado, I want to thank for companionship in the laboratory. To my dear friends, Inês Silva and Zenaide Alves, and my family, Jorge, Maria e Catarina Calado, I very much appreciate the love and support.

Abstract

Bacillus anthracis, a spore forming Gram (+) bacterium, is considered one of the most lethal biological weapons due to its highly pathogenic nature, easy production, preservation, and to the possibility of being aerosolized and sprayed. The fact that antibiotics are ineffective against the spores and the released toxins, makes it a serious threat [1,2].In addition, development of antimicrobial resistance has become a worldwide problem, as the impact of antibiotics is diminishing due to progressive rise of resistance to the available antimicrobial drugs [3].

It was previously described the importance of the bacteria membrane's integrity in its life - the cell envelope cannot change without significant consequences to the bacteria life. Also, the development of resistance becomes extremely difficult [4]. For this reason, the essentiality of cell membrane makes it a promising target for new antibiotics.

In order to target *B. anthracis* membrane, our research group has investigated the use of carbohydrate-based surfactants as potential antibiotics since these amphiphilic compounds are known to be able to interact with the cell membrane lipid bilayer [5]. Hence, a library of alkyl glycosides was synthesized varying deoxygenation pattern, alkyl chain, sugar stereochemistry, anomeric configuration and atom linking the alkyl chain to the saccharide moiety [6–10]. The compound that showed the best results was an *O*-glycoside, the dodecyl 4,6-dideoxy-α-D-*xylo*-hexopyranoside, which was active against *B. cereus*, *E. faecalis* and *B. anthracis* (strains: pathogenic, sterne and ovine) with MIC = 12.6 μM. Comparing to chloramphenicol, the control used in the biological assays, the MIC value revealed to be half of the MIC showed by the control (MIC = 25 μM). Also *C*-glycosides were found less toxic compounds on Caco-2 cells than the corresponding *O*- and *S*-glycosides [9].

The aim of the presenting dissertation was to explore the first synthetic route towards dodecyl 4,6-dideoxy-α-D-*xylo*-hexopyranoside, the *C*-glycoside analogue to the *O*-glycoside previously described. Three synthetic pathways were investigated, using either the naturally occurring D-glucose or its methyl glucoside as starting materials. When starting from D-glucose, it was regioselectively protected with a 4,6-*O*-benzylidene group while benzyl groups were protecting positions 1, 2 and 3. Since the reaction outcome of the acetal protecting group with *N*-iodosuccinimide was not successful possibly due to the reactivity of the benzyl protecting groups, other attempts were tried and the desired compound – the *C*-glycoside with the 4,6-dideoxy pattern (**19)** was obtained in 13% overall yield. Cytotoxicity tests are to be performed and biological assays are on-going in order to determine this *C*-glycoside efficacy towards *B. anthracis*.

Keywords

4,6-dideoxygenation

C-glycoside

Synthesis

Antimicrobial

Bacillus anthracis

Resumo

Bacillus anthracis, uma bactéria Gram (+) existente na forma de esporos, é considerada uma das armas biológicas de maior carácter letal devido à sua natureza altamente patogénica, à facilidade da sua produção e preservação bem como a possibilidade de os esporos serem pulverizados. O facto de os antibióticos não serem efetivos quando usados contra os esporos ou contra as toxinas libertadas pela bactéria, torna-a um problema sério [1,2]. Para além disso, o desenvolvimento de resistência a antibacterianos tornou-se um problema grave à escala mundial, com o impacto da evolução dos antibióticos a diminuir face ao aumento progressivo da resistência dos patógenos às terapêuticas disponíveis [3].

A importância da integridade da membrana bacteriana foi descrita anteriormente, onde se afirmou que o envelope celular não muda sem gerar consequências significativas na vida da bactéria. Ainda, o desenvolvimento de mecanismos de resistência torna-se extremamente difícil. Por esta razão, a essencialidade da membrana celular torna-a um alvo promissor para novos antibióticos [4].

Tendo a membrana da bactéria *B. anthracis* como alvo a atingir, o nosso grupo de investigação está focado no desenvolvimento de carboidratos surfactantes como potenciais antibióticos, uma vez que se sabe que este tipo de moléculas anfifílicas interage com a membrana lipídica das células [5]. Deste modo, foi sintetizada uma pequena biblioteca de *C*-glicósidos de alquilo com padrão de desoxigenação variável, diferentes cadeias alquílicas, estereoquímica do monossacárido, configuração anomérica e átomo que liga a cadeia alquílica ao glicósido [6–10]. O composto que demonstrou melhores resultados foi um *O*-glicósido, 4,6-didesoxi-α-D-*xylo*-hexopiranósido de dodecilo, que revelou ser ativo contra as bactérias *B. cereus*, *E. faecalis* e *B. anthracis* (estirpes: patogénica, sterne e ovino) com MIC = 12.6 μM. Comparando com os resultados demonstrados aquando do uso de cloranfenicol, controlo usado nos testes biológicos, o valor de MIC do *O*-glicósido revelou ser cerca de metade do valor de MIC do controlo (MIC controlo = 25 μM). Ainda, os *C*-glicósidos sintetizados demonstraram ser menos tóxicos para a linha celular Caco-2 do que os correspondentes *O*- e *S*-glicósidos [9].

O objetivo da dissertação apresentada foi o da exploração da primeira via sintética do composto 4,6-didesoxi-α-D-*xylo*-hexopiranósido de dodecilo, o *C*-glicósido análogo ao *O*-glicósido previamente descrito. Foram investigados três esquemas sintéticos, usando a D-glucose ou o seu análogo metilado como produtos de partida. O esquema sintético A partiu da D-glucose, cuja proteção dos grupos -OH livres foi conseguida com a introdução regiosseletiva do grupo 4,6-*O*-benzilideno e de grupos benzilo nas posições 1, 2 e 3. Uma vez que a redução do grupo benzilideno com *N*-iodosuccinimida não foi conseguida com sucesso, possivelmente devido à reatividade dos grupos benzilo, o esquema sintético B foi adotado. Após várias reações de proteção/desproteção dos hidroxilos da glícona, C-glicosilação da posição anomérica e elongação da cadeia alquílica, o derivado de glicósido desejado – o *C*-glicósido com o padrão de desoxigenação 4,6-didesoxi (**19**) foi obtido com um rendimento total de 13%. Os resultados dos testes de citotoxicidade são esperados de modo a confirmar a hipótese, inicialmente proposta, de que o *C*-glicósido é menos tóxico que o seu análogo *O*-glicósido. Além disso, os testes biológicos estão em curso para que seja determinada a eficácia deste *C*-glicósido contra a bactéria *B. anthracis*.

Palavras-chave

4,6-dideoxigenação

C-glicósido

Síntese

Antimicrobianos

Bacillus anthracis

Table of contents

List of Figures

List of Schemes

List of Tables

List of symbols and abbreviations

Ac – Acetyl
Ac_2O – Acetic anhydride
ACN – Acetonitrile
AIBN – Azobisisobutyronitrile
AMR – Antimicrobial resistance
Aq – Aqueous
ATP – Adenosine triphosphate
AZT – azidothymidine
B. - *Bacillus*
Bn - Benzyl
Br – Broad
Bz – Benzoyl
c – Concentration in g/mL
COSY - COrrelated SpectroscopY
C_q – Quaternary carbon
CSA – Camphorsulphonic acid
Cy – Cyclohexane
d - Doublet
dd – Doublet of doublets
DCC – *N,N´*-dicyclohexylcarbodiimide
DCE – 1,2-Dichloroethane
DCM – Dichloromethane
DIBAL-H – Diisobutylaluminum hydride
Dipea – Diisopropylethylamine
D*i*PPF – 1,1´-Bis(diisopropylphosphino)ferrocene
DMAP – 4-dimethylaminopyridine
DMF – Dimethylformamide
DNA – Deoxyribonucleic acid
dt – Doublet of triplets
E. – *Enterococcus*
Eq – Equivalent
et. al. – *et alia*
EtOAc– Ethyl Acetate
FDA – Food and Drug Administration
i.e. – *id est*
IUPAC – International Union of Pure and Applied Chemistry
Hex – Hexane
HIV – Human Immunodeficiency Virus
HMBC – Heteronuclear Multiple Bond Correlation
HSQC - Heteronuclear Single Quantum Correlation
IC_{50} – Half Maximal Inhibitory Concentration
J – Coupling constant
LG – Leaving group
m – Multiplet
m-CPBA - *meta*-Chloroperoxybenzoic acid
MDR – Multiple drug resistance
Me – Methyl
MeOH – Methanol
MIC – Minimum Inhibitory Concentration
M.p. – Melting point
MRSA – Methicillin-resistant *Staphylococcus aureus*
NaOMe – Sodium Methoxide
NBS – *N*-Bromosuccinimide
NIS – *N*-Iodosuccinimide
NMR – Nuclear Magnetic Resonance
OM – Outer membrane
p.a. – Pro analysis
PE – Phosphatidylethanolamine
Piv – Pivaloyl
Ph – Phenyl
ppm – Parts per million
p-TSA – *para*-toluenesulfonic acid
Py – Pyridine
s – Singlet
S. – *Staphylococcus*
Sp. – Specie
Rf – Retention factor
RNA – Ribonucleic acid
t – Triplet
TBAF – Tetrabutylammonium fluoride
TBAHS – tetrabutylammonium hydrogen sulphate
TBDMSCl – *tert*-butyldimethylsilyl chloride
TBDPSCl – *tert*-butyldiphenylsilyl chloride
TBSOTf – *tert*-butyldimethylsilyl trifluoromethanesulfonate
td – Triplet of doublets
tert - Tertiary
Tf_2O – Trifluoromethanesulfonic Anhydride
THF – Tetrahydrofuran
TLC – Thin Layer Chromatography
TMSCl – Trimethylsilyl chloride
TMSOTf – Trimethylsilyl trifluoromethanesulfonate
TPHB – Triphenylphosphane hydrobromide

VRSA – Vancomycin-resistant *Staphylococcus aureus*
Vs. – *Versus*

$[\alpha]_D$ - Specific optical rotation
δ - Chemical shift

1 Introduction

1.1 Carbohydrates

Carbohydrates are one of the most abundant molecules on Earth and essential to life prosperity. In early Earth life, these molecules played a key role in the evolution of the living organisms.

In the presence of sun light, during the photosynthesis process, it is possible to combine water and carbon dioxide to give rise to carbohydrates and molecular oxygen (equation 1.1). The energy, stored as $C_6H_{12}O_6$ structure type, is then usable by non-photosynthesizing organisms in processes known as glycolysis and respiration. It is suggested that in ancient earth, the amount of available oxygen was scarce and therefore the carbohydrates were broken down through anaerobic glycolysis, to form adenosine triphosphate (ATP) and lactic acid (equation 1.2). As only a limited amount of energy was available - 2:1 (ATP/ $C_6H_{12}O_6$), life on earth remained primitive. However, in the course of time, with the increase of the concentration of molecular oxygen in the atmosphere, the living organisms evolved to completely oxidize the carbohydrates, through the respiration process. As a consequence, the amount of usable energy increased significantly - 38:1 (ATP/ $C_6H_{12}O_6$) (equation 1.3), leading to a burst in the number and complexity of living organisms.

In today's life, certain carbohydrates provide up to 60% of the total of calories of a human diet, being glucose extremely important, with blood concentration of about 1g/L[11].

$$6\ CO_2 + 6\ H_2O \xrightarrow[\text{photosynthesis}]{h\nu} C_6H_{12}O_6 + 6\ O_2 \qquad 1.1$$

$$C_6H_{12}O_6 \xrightarrow{\text{anaerobic glycolysis}} \text{2 lactic acid} + 2\ ATP \qquad 1.2$$

$$C_6H_{12}O_6 \xrightarrow{\text{respiration}} 6\ CO_2 + 6\ H_2O + 38\ ATP \qquad 1.3$$

Apart from its importance as energy suppliers, carbohydrate also exist as polymers, which serve as structural components of bacteria and plants' cell walls, being the case of cellulose. Other carbohydrates are crucial in biological processes as they mediate cellular adhesion and recognition, as mentioned in section 1.2.3, page 11, where it will be discussed the use of carbohydrates as antibiotics.

The study of the carbohydrates arises from the 19th century, where it was thought that they were carbon hydrates, being their empirical composition expressed by the general formula $C_n(H_2O)_n$. Later on, it was found that carbohydrates are, in fact, polyhydroxy aldehydes and ketones but their derivatives were also included in this class of compounds [11,12].

In fact, according to IUPAC Recommendations, the generic term "carbohydrate" includes monosaccharides, oligosaccharides, polysaccharides and substances derived from monosaccharides' carbonyl group reduction, oxidation of one or more terminal groups or replacement of one or more hydroxy groups by a hydrogen atom or an amino, thiol or other heteroatomic group. The term "sugar" is commonly used when referring to monosaccharides and oligosaccharides with low molar mass[12].

1.1.1 -D and -L configuration

Emil Fischer gave a major contribution to this field of organic chemistry by identifying, characterizing and synthesizing monosaccharides. Very briefly, with the introduction of the concept of stereochemistry, by van't Hoff and Le Bel in 1874, Fischer was able to understand carbohydrates isomerism and proposed what is known as the Fischer projection. This projection consists in representing monosaccharides through a central carbon chain, with the carbonyl group on top and the hydroxy groups as substituents, pointing left or right, along the vertical chain (see Figure 1.1)[11–14].

Melting point and optical rotation were the essential techniques used to identify monosaccharides. In the case of optical rotation, dextrorotation occurs when the compound analysed deviates the plane-polarized light to the right (expressed as (+)) and levorotation occurs when the plane-polarized light is deviated to the left (expressed as (-))[13].

Only being confirmed later on, Fischer proposed that the dextrorotatory glucose (D-glucose) would have the hydroxy group in C-5 pointing to the right in the carbon backbone (see Scheme 1.1). In 1906, Rosanoff elected glyceraldehyde as the reference molecule to do the D- and L- attributions, *i.e.*, any sugar derived from D-glyceraldehyde by increasing the length of the sugar backbone belongs to the D-series, whereas any sugar derivable from L-glyceraldehyde by increasing the length of the sugar backbone belongs to the L- series (see Figure 1.1). Although the convention proposed by Rosanoff continues in use, now it is known that a compound with D- configuration may not be dextrorotatory[12,13]. When accessing the absolute configuration of a sugar with two or more chirality carbons, the last chiral carbon is used as term of comparison with glyceraldehyde (see Figure 1.1 for numbering of carbons in Fischer projection)[13,14].

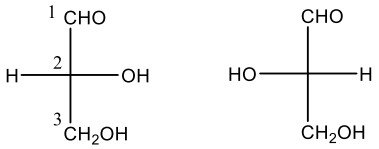

Figure 1.1. From left to right, D- and L-glyceraldehyde.

1.1.2 Mutarotation

In 1846, the term "mutarotation" had been introduced by Dubrunfaut, as he realized that the optical rotation of a pure enantiomer of glucose changes with time. He observed that a freshly prepared solution of α-D-glucopyranose in water has a specific rotation of about +112º, which decreases with time to +52º. Likewise, a freshly prepared solution of β-D-glucopyranose in water has a specific rotation of about +19º, which also decreases with time to +52º. This value does not correspond to a new structure of glucose, as initially thought, but to the mixture of both α and β isomers in equilibrium in the solution (see Scheme 1.1) [12,13].

Still in late 19th century, von Baeyer and Tollens also suggested the existence of two cyclic forms of the D-glucose, resulting from the nucleophilic attack of one of the hydroxy groups to the carbonyl moiety, giving rise to the two isomeric forms (α and β). Depending hydroxy group attacking the carbonyl, glucose would cyclize as a five or a six-membered ring (see Scheme 1.1) [13,14].

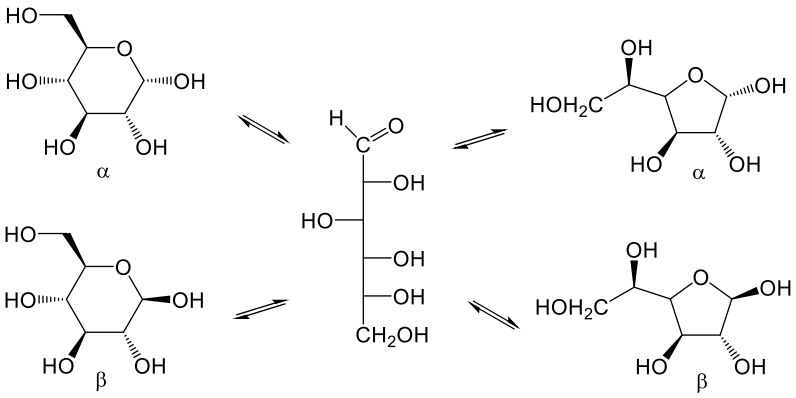

Scheme 1.1. Representation of the equilibria causing D-glucose mutarotation (equilibrium between acyclic form and the α and β anomers of D-glucose of both pyranose and furanose forms) [12,13].

In order to facilitate the representation of sugars, in 1926, Haworth suggested a simpler representation of a six membered ring glucose – what is now known as Haworth projection, shown in Figure 1.2. In 1955 another representation, still in use today, was proposed by John A. Mills (see Figure 1.2) [13,14].

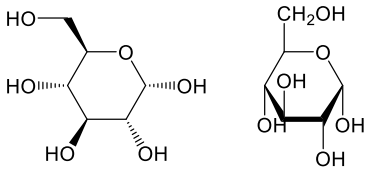

Figure 1.2. From left to right, representation of Mills and Haworth projection of α-D-glucopyranose. In the first one, the ring is visualized in the plane of the paper, while the substituents are represented with "wedge" (above) or dashed (below) notation. In the second one, the ring is viewed front edge-on the paper, across the C2-C3 wedge-bond, with the substituents pointing "up" or "down" the hexagon.

It is known that when chemical species are in rapid equilibrium, the concentration of each species depends on its relative energy. In fact, D-glucose exists as a hemiacetal ring and its isomers, depicted in Scheme 1.1, exist in equilibrium in different ratio. The amount of the pyranose form is much higher than the amount of the furanose form, where its equilibrium concentration is only about 0.11% and 0.28% (α and β-furanose respectively) of the total equilibrium concentration of glucose. On its turn, the acyclic form only accounts for a trace of the total glucose (about 0.004%). And even the two pyranose anomers exist in different proportions, due to their different stability, being the α and β, 37.64% and 61.96% respectively [15,16].

The low thermodynamic stability of the open chain explains its appearance in vestigial quantity as well as the preference for the six-membered ring form over the five-membered ring form, where the torsional strain tends to be minimized. As for entropy, it is more favourable to occur an intramolecular reaction than an intermolecular one, explaining the cyclization of the sugars instead of the nucleophilic attack by a hydroxy group of one molecule to the carbonyl moiety of another molecule. Also, the β anomer is more stable since all the substituents in the sugar are in equatorial position, minimizing electrostatic repulsions between the ring's substituents, whereas in the α anomer, the hydroxy group in the anomeric position is in axial position [13–16]. Note that for pyranose rings, it is quite common that the α anomer has higher stability than the β one, being this stabilization effect named as anomeric effect (mentioned in page 6).

1.1.3 Conformation

The stability of the pyranose forms is related to their special rearrangement. In the equilibrium between D-glucopyranose anomers and D-glucofuranose anomers, the most stable form is the β-D-glucopyranose showing the $^4C_1$ chair conformation, in which all hydroxy groups are in equatorial orientation (see Figure 1.3).

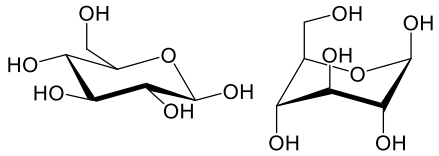

Figure 1.3. Representation of the $^4C_1$ and $^1C_4$ chair conformation of β-D-glucopyranose (from left to right, respectively)

In early 1900, Hassel demonstrated that the cyclohexane ring was not planar but it showed a non-planar shape, similar to a chair. Now it is well known that there are several conformations of cyclohexane in rapid equilibrium, the boat conformation (B), the chair conformation (C) and another degenerate chair conformation, where there is interchange of the axial/equatorial bonds [15].

The carbon-heteroatom bond length is shorter than the carbon-carbon bond length, as well as the carbon-heteroatom-carbon angles are generally smaller than the corresponding C-C-C angles. As a consequence, the substituents in a heterocycle have higher preference for the equatorial positions when compared to the cyclohexane ring, in order to minimize electrostatic repulsions, explaining the preference for $^4C_1$ conformation over the $^1C_4$ conformation (see Figure 1.3) [17].

However, being the chair conformation the spacial rearrangement preferred by D-glucopyranose, there are other possible conformations for pyranose rings – half chair (H) and skew (S). Although worth mentioning, these last conformations are higher energy forms, only existing in vestigial quantity, when converting the chair conformations in one another. In the case of furanose ring, there are two main possible conformations – envelop conformation (E) and twist conformation (T) [15,16].

Lemieux and Karplus suggested, by ^{1}H NMR, that it is possible to distinguish both $^4C_1$ and $^1C_4$ chair conformations when measuring the coupling constants between H-2 and H-3. Owing to the relationship between the magnitude of the coupling constant and the size of the torsional angle between vicinal protons, in the first form, $^3J_{2,3}$ is higher (in the order of 9Hz – 10Hz) since H-2 and H-3 are in *trans* diaxial position, with a dihedral angle near 180º while in the second form this coupling constant should be between 1Hz – 2 Hz. This rule is applied when determining the chirality centers' configuration of the sugars using NMR analysis (see Figure 1.4) [15,16].

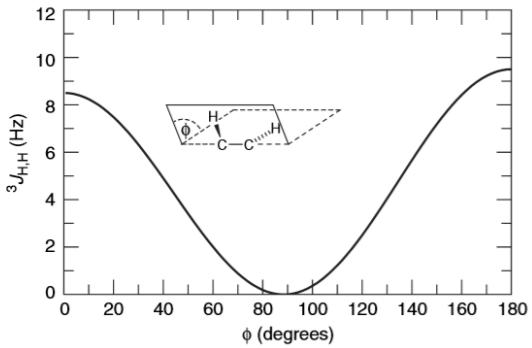

Figure 1.4. Representation of the coupling constant (in Hertz) of vicinal protons in function of their dihedral angle (in degrees), proposed by Karplus. Figure adapted from the literature [11].

1.1.4 Anomeric effect

One of the most important observations made when studying the carbohydrates was that the presence of the endocyclic oxygen in the monosaccharide ring deeply influences the anomeric position, being quite common the preference for the formation of the α anomer over the β anomer. This phenomenon was named as anomeric effect, in 1958, by Lemieux [15].

Briefly, this effect has been explained using an electrostatic and a stereoeletronic interpretation.

In 1955, it was first proposed that the existence of a repulsive dipolar interaction between the lone pair of electrons of the endocyclic oxygen and the exocyclic heteroatom in equatorial position would be relieved if the substituent adopted an axial configuration (see Figure 1.5).

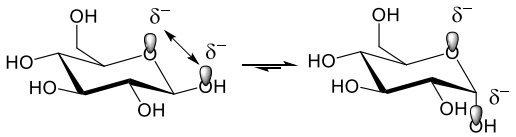

Figure 1.5. Electrostatic repulsion between the endocyclic heteroatom and the substituent in β and α configuration (from left to right, respectively) in a $^4C_1$ conformation. Adapted from the literature [17].

More recently, it has been suggested the importance of a nonclassical CH···X hydrogen bond between the axial group at C-1 and the *syn*-axial hydrogens in C-3 and C-5 in the stabilization of the axial anomer (see Figure 1.6 a) [17–19]. In fact, the magnitude of the anomeric effect is dependent on the solvent used, as more polar solvents stabilize the equatorial configuration. Also, the electronegativity of the substituent is decisive, being the magnitude of this effect increased in the presence of more electronegative atoms [17,18]. On the other hand, the reverse anomeric effect occurs when the anomeric substituent has lower electron density, where the β anomer is preferentially formed.

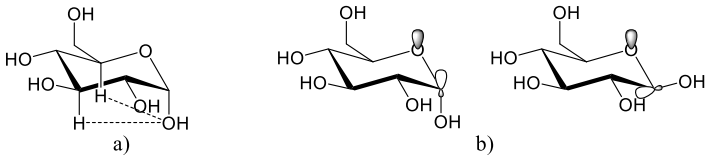

Figure 1.6. a) Representation of the nonclassical CH···X hydrogen bond between the axial group at C-1 and the syn-axial H-3 and H-5, adapted from the literature [18,19]. b) Representation of the stereoeletronic interpretation of the anomeric effect in a $^4C_1$ conformation, adapted from the literature [17].

On the stereoeletronic interpretation, this effect is explained by the hyperconjugative interaction involving electron delocalization from the endocyclic oxygen to the adjacent C1 – X antibonding orbital. The stabilization effect arises from the fact that, in the axial anomer, the orbital with the lone pair of electrons in the oxygen and the mentioned antibonding orbital are antiperiplanar (see Figure 1.6 b). Also important is the delocalization of the hydrogen (H – C – X) electron density into X, being a major contribution to the anomeric effect. It results from the lengthening of the C – X bond, in order to minimize the repulsion with the ring atom and favouring the interaction between the endocyclic oxygen and a more positive hydrogen. Experimentally, it can be measured the lengthening of the C – X bond and the shortening of the C – O bond in cases that display an anomeric effect [11,13,14,17].

1.1.5 Glycosylation

Carbohydrates exist as mono-, oligo- and polysaccharides or associated to proteins or lipids, glycoproteins and glycolipids respectively. Hence, it is implied a coupling reaction between a glycosyl donor and a glycosyl acceptor to form a new glycoside.

As referred in IUPAC Recommendations, glycosides are defined as mixed acetals/ketals derived from cyclic forms of monosaccharides, being included derivatives in which the anomeric hydroxy group has been replaced by a -OR, $-NR^1R^2$, -SR, -SeR, or $-CR^1R^2R^3$ group, where R is arbitrary [12], while when replaced by $-NR^1R^2$, or $-CR^1R^2R^3$ groups, these compounds should not be named as glycosides since their reactivity is not similar to that of acetals.

In a typical glycosylation reaction, one of the building blocks (glycosyl donor) has the anomeric position substituted with a good leaving group, while the other (glycosyl acceptor) has one functional group that will act as nucleophile (independently of being sugar or non-sugar derived) (see Scheme 1.2) [11–15]. In the final glycoside, both building blocks are linked through a glycosidic bond and the final glycoside is named either as *O*-glycoside (-OR), thioglycoside (-SR), selenoglycoside (-SeR), while glycosylamine ($-NR^1R^2$) and *C*-glycosyl compounds ($-CR^1R^2R^3$) are generic terms used for the latter compound families. It is common to refer to the carbohydrate residue as glycone, and to the glycosyl acceptor residue, aglycone (in cases where the nucleophile is not a monosaccharide) [12].

All of the above described glycosidic bonds have different susceptibility to hydrolysis, typically, *C*-glycosyl compounds are hydrolysis stabile, as ethers. *C*-glycosyl compounds will be discussed in section 3.1.2, page 24.

In 1983, Emil Fischer made an innovative breakthrough when activating the hemiacetal function of glucose and replacing the anomeric hydroxy group with a methoxy group, using methanol in the presence of an acid catalyst. This work was not pioneer, as methyl glucoside had been already synthesized before, however it was performed in an unprotected sugar, which was a notorious mark [20]. In fact, one of the major challenges in carbohydrate synthesis is the control of regioselectivity, since there are multiple hydroxy groups, able to react.

In order to overcome that issue, generally, all the functional groups in both glycosyl donor and acceptor are temporarily masked with adequate protecting groups, except for the reactant moieties. There are, however, cases of glycosylation reactions using totally or partially unprotected glycosyl donors/acceptors, under specific reaction conditions [20–22]

The other major challenge is the stereoselectivity control, since reaction leads to two stereoisomers due to the formation of a new chirality centre. This, however, can be managed with the correctly chosen carbohydrate protecting groups and leaving group, catalyst, solvent and temperature [3,20,23–25].

Although not completely understood yet, it is agreed that glycosylation reactions undergo either a S_N1 or S_N2 type mechanism (see Scheme 1.2). Usually, prior to nucleophilic attack, there is displacement of the anomeric leaving group (-LG), assisted by the catalyst in solution. It is then formed an intermediate oxycarbenium ion. There are cases where the glycosyl donor is equipped with an acyl derived group in position 2, which in turn can participate in the reaction by forming a cyclic acyloxonium intermediate. This intermediate exists in rapid equilibrium with the oxycarbenium ion, stabilizing it. Hence, the following nucleophilic attack occurs either on the top or the bottom face of the sugar, depending on the steric hinderance caused by the new intramolecular cycle – the neighbouring group effect. In the case of D-glucose, since the substituent in C-2 is in an equatorial position, the attack would occur on the top face, forming the β anomer as major product [20–23,25].

The described mechanism is similar to a typical S_N2 reaction, however, when the stereocontrol of the reaction is diminished, for instance, due to poor nucleophilic nature of the glycosyl acceptor or weak assistance of the substituent in C-2, the glycosylation reaction may adopt a mechanism similar to an S_N1 reaction, with the nucleophilic attack direct to the oxycarbenium intermediate. In this case, the anomeric effect is prevalent, originating the α isomer as major product (see section 1.1.4, page 6 for anomeric effect enlightenment) [20,25].

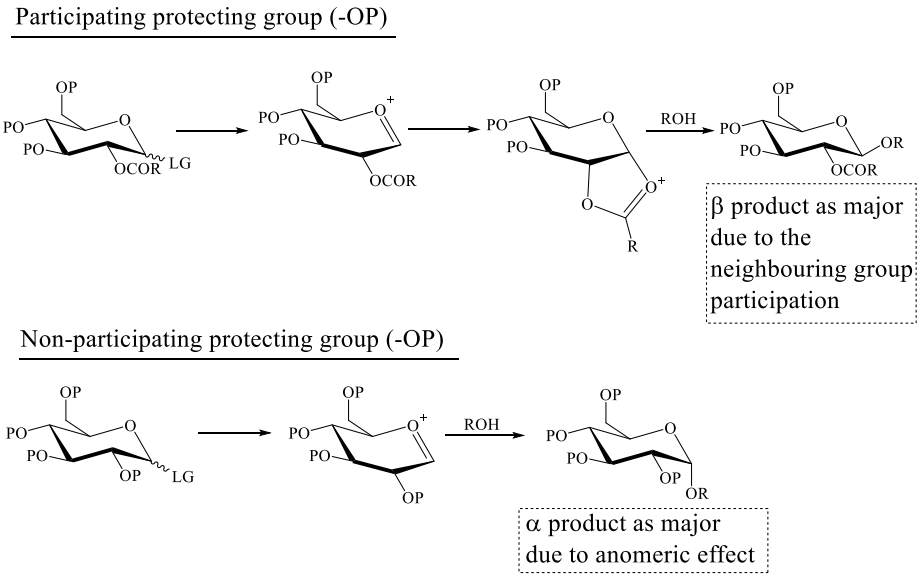

Scheme 1.2. Strategies for anomeric stereoselective control, exemplified for the formation of an O-glycoside. P refers to a generic protecting group, LG stands for leaving group and R for a generic group function. Adapted from the literature [20].

1.2 Antibiotics

The control of bacterial infections has been well documented in the past centuries in Greece, Egypt and China. Nevertheless, until mid-20th century, bacterial infections that we now consider straightforward to treat – such as pneumonia or diarrhoea – that are caused by bacteria, caused human death in the developed world [3,26].

In 1928, Alexander Fleming transformed medicine with the discovery of the first antibiotic – the penicillin. After struggling with purification issues, in the 1940s, the first prescription of penicillin was made. Later, it was called the "wonder drug" as, coinciding with the World War II, it became the treatment of choice amongst the bacterial infected soldiers, saving lives [3,26].

Antibiotics are bacterial or fungal metabolites which are able to inhibit the growth of other microorganisms, including natural, semi-synthetic or synthetic antibacterial substances. They can be classified as bactericides – directly killing the microorganisms or bacteriostatic – slowing down bacteria growth/reproduction [5,27].

Despite this, shortly after penicillin's discovery, in 1940, Abraham and Chain reported that a specific *Escherichia Coli.* strain was able to inactivate this antimicrobial compound by producing penicillinase [28]. Over time, several strains of other types of bacteria also became resistant to penicillin. For instance, by 1960, 80% of community and hospital acquired strains of *Staphylococcus aureus* were penicillin resistant. By 2003, more than 90% of staphylococcal isolates produced penicillinase, regardless of the clinical setting [26,29].

The imprudent and excessive use of antibiotics in both humans and animals, allied with natural resilience mechanism of bacteria, rely as the major cause of resistance evolution – the sensitive bacteria are killed while resistant pathogens persist and reproduce through different mechanisms, thriving through natural selection [3,26].

Hence, the emergence and propagation of the resistant bacteria strains led to the development of novel types of antimicrobials. Throughout the past 75 years, several classes of antibiotics were identified – β-lactams (where it is included the several types of penicillin), sulphonamides, tetracycline, glycopeptides, phosphonates, lipopeptides amongst others. However, bacteria have developed resistance to them, through different mechanisms of resistance – either the antibiotic is pumped out by the bacteria by efflux pumps on the cell wall or there is enzymatic breakdown/modification of the antibiotic or even modification/multiplication of the target [3,26].

Antimicrobial resistance (AMR) is a serious global threat and, unfortunately, the impact of antibiotics is now diminishing due to the progressive rise of resistance, and this is observed amongst all antimicrobial drugs. There are bacterial species resistant to all known antibiotics (multidrug-resistant bacteria - MDR), leaving both humans and animals vulnerable to common infections [3]. Hence, the development of new antimicrobials with novel mechanisms of action is key.

1.2.1 Gram-positive and Gram-negative bacteria

By 1884, Christian Gram classified nearly all bacteria in two large groups – Gram-positive and Gram-negative, based on the structural differences of their cell envelope. Commonly referred as examples, are *Escherichia coli*, a Gram-negative bacteria and *Staphylococcus aureus*, a Gram- positive bacteria [28,30].

The outer membrane (OM) in Gram (–) bacteria is a lipid bilayer essentially composed by glycolipids, principally, lipopolysaccharides (LPS), which are inflammation mediators to the human innate system. The OM plays a significant role in protecting the bacteria from the exterior environment, indirectly stabilizing the inner membrane. For this reason, the peptidoglycan wall is very thin, although, because of its rigidity, it defines the cell shape [28,30].

On the other side, Gram (+) bacteria lack the OM and in turn have a thicker peptidoglycan wall. In this wall, and accounting for up to 60% of the mass of Gram (+) bacteria, there are teichoic and lipoteichoic acids, polysaccharides covalently attached to the peptidoglycan and anchored to membrane-embedded glycolipids. These polymers play a major role in the membrane integrity [28,30].

The bacterial cell membrane is independent of the cell's metabolic status, however it is crucial for cell survival as it regulates homeostasis and houses vital proteins. Hence, the cell envelope cannot change without significant consequences to the bacteria life and also, the development of resistance becomes extremely difficult. For this reason, the essentiality of cell membrane makes it a promising target for new antibiotics. Also, molecules targeting cell membrane may act together with conventional drugs, as they can compromise cell envelope permeability and integrity, increasing drugs' efficacy [4].

1.2.2 *Bacillus anthracis*

Bacillus anthracis (*B. anthracis*), the causative agent of anthrax, is a Gram-positive spore forming, non-motile bacterium that belongs to *Baccillus cereus* (*B. cereus*) *sensu lato* group. This bacterium exists as two forms, as spores (outside the host) or as vegetative cells (inside the host)[31]. The spore is normally encountered in the soil, where it can remain, in anaerobic conditions, viable for decades, as it is resistant to extreme environmental conditions, such as high temperature, pressure, pH, UV and nutrient deficit. Its half-life is estimated of about 100 years [31–33].

In the worst cases, the cycle of life starts with spores' germination as they enter the hosts' bloodstream, a nutrient rich media, where they regain metabolism and start vegetative growth, with further bacteria multiplication. *B. anthracis'* virulence is controlled by the presence of a poly-γ-D-glutamic acid capsule and the later released tripartite toxin. In fact, a specific strain of *B. anthracis* which have no capsule but carries the toxin, is considered avirulent and it is even used in the production of vaccines. The capsule itself is not toxic, however it contributes significantly in establishing the infection as it mimics the host immune system, escaping phagocytes ability to engulf and destroy bacteria. The disease spread is then controlled by the bacteria's toxin releasing. The infection may take only a few days to be lethal to the host organism, whose infected blood and body fluids leak to the exterior through natural orifices. Once outside the host, the vegetative cells convert into spores once again [31].

Although this disease mainly affects wild and domestic herbivore animals in countries where widespread vaccination is not practiced, it also infects humans through contact with infected livestock or animal products, such as their skin, hide, meat or bones[31]. In Africa, Asia and South America, anthrax infection remains a severe problem, as humans frequently butcher and eat infected animals [32]. The infection can be done through cutaneous, gastrointestinal or respiratory routes, each with different mortality rates [31].

Owing to its highly pathogenic nature, to the easy production and preservation and to the possibility of being aerosolized and sprayed, *B. anthracis* is considered one of the most lethal biological weapons. In fact, methodologies may have been developed for it to be used as a bioweapon in world war I and II. More recently, in 2001, *B. anthracis* was used as a bioterrorism agent – letters deliberately infected with *B. anthracis* were sent to different notables in USA, affecting 22 people [31–34].

Anthrax is nonfatal in early stages, being treatable with long-term intravenous treatment with quinolones and tetracyclines [4]. However, it has been reported the existence antibiotic resistant strains of *B. anthracis*, namely to ciprofloxacin, a first line treatment for bacterial infections. What is more, antibiotics in the market are ineffective against the spores and the released toxins [1,2].

1.2.3 Antibacterial carbohydrates

Carbohydrate-based antimicrobials either occur naturally or are semisynthetic and the sugar moiety may be the main structural part, such as in the case of aminoglycosides and nucleosides, or it may be attached to a non-carbohydrate core structure, for instance, in glycopeptides and macrolides [5,35].

Structurally, aminoglycosides consist of a six-membered ring aminocyclitol to which are linked several amino glycosides (see streptomycin's structure in Figure 1.7 as example). They are classified as bactericidal antibiotics, produced by strains of *Actinomycetes* species and active against Gram-negative bacteria. The general mechanism consists in inhibiting protein synthesis by binding to a ribosomal unit, promoting mistranslation and eliminating proofreading (error-correcting processes) [4]. More recently, it has been detected bacterial membrane damage by streptomycin, a type of aminoglycoside [36]. Although this type of antimicrobials is not first line treatment for certain infections, by 2004, it was observed that 80% of hospital-associated methicillin-resistant *S. aureus* (MRSA, a *S. aureus* strain multiple drug resistant common in hospitals) infections have resistance to multiple aminoglycosides [37]. Despite this, efforts are being made in the structural modification of aminoglycosides in order to overcome drug resistance issues. For instance, FDA recently approved the use of plazomicin (see Figure 1.7) in complicated infections caused by the multidrug resistant *Enterobacteriaceae* [38,39].

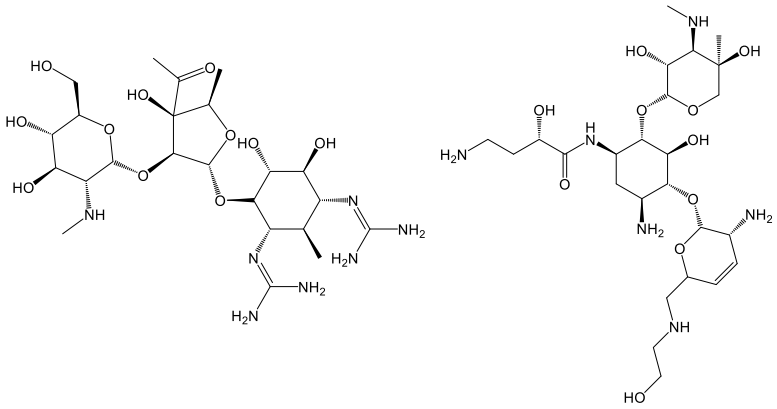

Figure 1.7. From left to right, streptomycin and plazomicin's structure, two aminoglycosides.

The nucleoside analogues, in turn, are a combination of parts of natural nucleosides conjugated with additional structures, amino acids, fatty acids, disaccharides or higher sugars, with the combination having antibacterial properties against Gram-positive and Gram-negative bacteria [5,40–42]. These compounds primarily target a specific translocase (MraY) essential to peptide-glycan biosynthesis and

consequently cell-wall formation [40–42]. Also, due to the fact that nucleoside analogues mimic endogenous nucleosides, they may be incorporated in the bacterial DNA/RNA and stop chain elongation, which is the case of Zidovudine (AZT, normally prescribed as clinical therapy for HIV, see Figure 1.8) when used as antimicrobial agent against *Enterobacteriaceae* species [41]. This class of compounds has attracted attention due to their high efficacy against various pathogenic bacteria including MRSA, and vancomycin-resistant *Enterococcus*. It is worth saying that efforts are being made in order to expand the nucleoside-based antimicrobials repertoire[41].

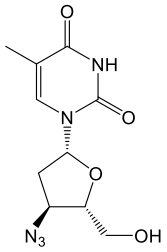

Figure 1.8. Structure of the nucleoside analogue Zidovudine (AZT)

Glycopeptides are another type of carbohydrate based antimicrobial compounds, active against Gram-positive bacteria. Their structure comprises a cyclic peptide *O*-glycosylated with mono- or disaccharides. One of the most well-known compounds of this class is vancomycin (see Figure 1.9), isolated from *Amycolatopsis orientalis*. The significant lag time between its discovery and the appearance of bacteria resistance, due to the lack of cross resistance with other classes of antibacterial agents made it an increasingly prescribed therapeutic option. Glycopeptide antibiotics operate by inhibiting the assembly of the cell wall peptidoglycan – they bind to a specific peptidoglycan precursor, preventing its incorporation into the essential structural cell wall component [5,43]. Although vancomycin has been the mainstream therapeutic for MRSA infections for decades, other generations of glycopeptides were developed. For instance, in 2014, oritavancin (see Figure 1.9), an active compound over MRSA and VRSA (vancomycin-resistant *S. aureus*), was approved by FDA for the treatment of skin infections [4].

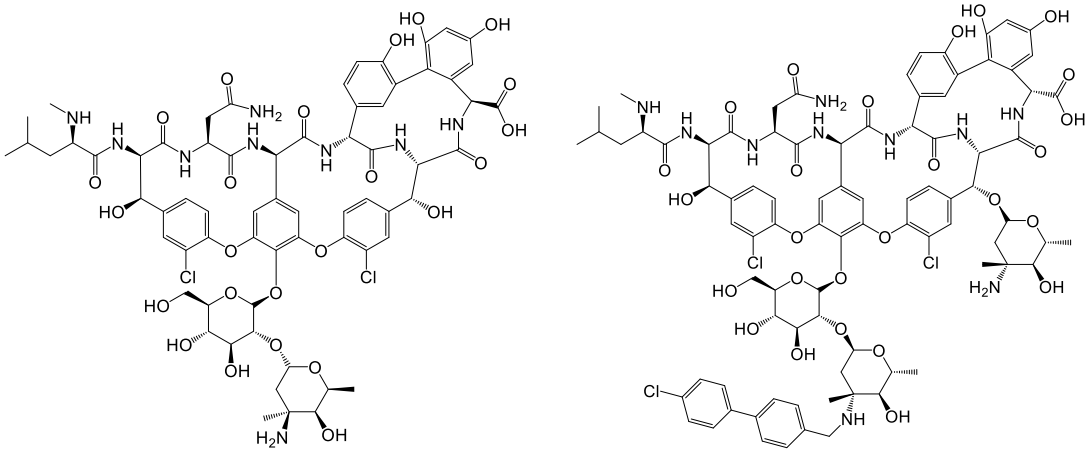

Figure 1.9. From left to right, structure of vancomycin and oritavancin.

Finally, the macrolide class of antimicrobials comprises compounds with a macrocyclic lactone *O*-glycosylated with one or more deoxy sugars, being either 12-, 14-, 15- or 16-membered ring macrolides. They are effective against Gram-positive bacteria, have only limited activity against Gram-negative

bacteria and are potent antifungal compounds, namely the polyene macrolides [4]. On the first generation of macrolides, erythromycin (see Figure 1.10), a 14-membered macrolide, isolated from the *Streptomyces erythraeus* or *Arthrobacter*, is the best-known compound. Due to poor bioavailability, structural changes were made, and other derivatives were synthesized, such as azithromycin (see Figure 1.10). As the problem of drug resistance remained, the search for other derivatives continued and today the only therapeutic macrolide on the marked is telithromycin (see Figure 1.10) [44]. Regardless of compound's generation, their antibacterial properties are given by the ability of binding to the prokaryotic ribosome and preventing peptide synthesis [5,44].

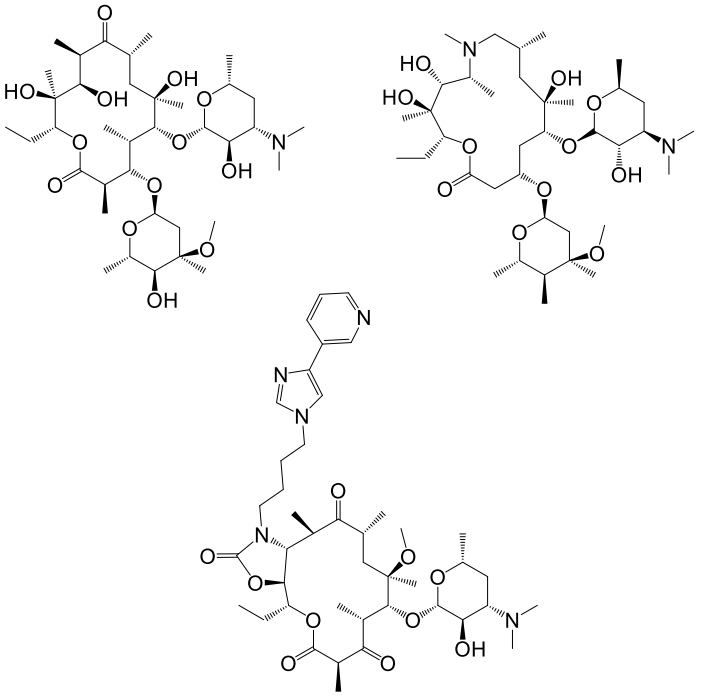

Figure 1.10. Above, from left to right, structure of erythromycin and azithromycin. Below, structure of telithromycin.

1.2.4 Novel carbohydrate-based antimicrobials

Over the years, sugar-based surfactants became an interesting class of compounds, as they have a wide range of applications, from detergents to agrochemicals or explosives. Their low toxicity became relevant in its application not only in the food and cosmetic industry but also in the pharmaceutical field [6]. In fact, another emerging class of potential synthetic antibiotics are these amphiphilic molecules [4,6-8].

These compounds comprise a long hydrophobic tail linked to a carbohydrate hydrophilic moiety through an ester, amine, amide or glycosidic linkage and are known to be able to interact with the cell membrane lipid bilayer [5], thus being worthy of further studies in the field of membrane-targeting antibiotics.

In fact, our research group has been focused in the study of structure – activity correlation of alkyl glycosides as antimicrobial compounds. Several new compounds, belonging to the D series and to the L series with α and β configurations were synthesised with different sugar deoxygenation patterns, comprising also different alkyl chains (see Figure 1.11).

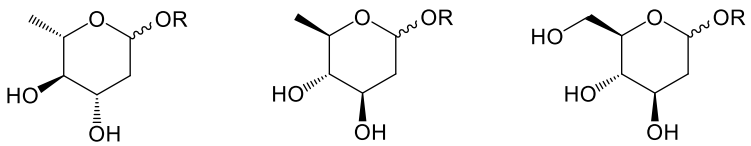

R1) α, $R_2 = C_8H_{17}$
R2) β, $R_2 = C_8H_{17}$
R3) α, $R_3 = C_{12}H_{25}$
R4) β, $R_3 = C_{12}H_{25}$

R5) α, $R_2 = C_8H_{17}$
R6) β, $R_2 = C_8H_{17}$
R7) α, $R_3 = C_{12}H_{25}$
R8) β, $R_3 = C_{12}H_{25}$

R9) α, $R_2 = C_8H_{17}$
R10) β, $R_2 = C_8H_{17}$
R11) α, $R_3 = C_{12}H_{25}$
R12) β, $R_3 = C_{12}H_{25}$

Figure 1.11. Structure of the synthesized compounds by Rauter et. al.*. From **R1 - R4**, 2,6-dideoxy-L-arabino-hexopyranosides, from **R5 - R8**, 2,6-dideoxy-D-arabino-hexopyranosides and from **R9 - R12**, 2-deoxy-D-arabino-hexopyranosides* [6–8].

The antimicrobial activity of compounds **R1** – **R12** was primarily accessed by the paper disk diffusion method followed by the measurement of the minimum inhibitory concentration value (MIC) of the most promising compounds (see [6–8] for more detail). The compounds were tested against several pathogens and were active against Gram (+) bacteria, being the best results shown with *B. anthracis*, *B. cereus* and *B. subtilis*, *E. faecalis* and *Listeria monocytogenes.*

The most promising MIC values were given by the dodecyl 2,6-dideoxy-L-*arabino*-hexopyranoside **R3** when tested against *B. cereus* and *B. subtilis*, with MIC values (MIC = 7.8 μM in both cases) close to the ones of the control (MIC = 3.1 μM and 6.3 μM against *B. subtilis and B. cereus* respectively). Also, this compound proved efficient against *E. faecalis* (MIC = 15.6 μM) and *Listeria monocytogenes* (MIC = 31.3 μM) [7].

The compounds were also tested against three different strains of *B. anthracis* species. In this case, sugar derivatives with the 2,6-dideoxy pattern bearing a dodecyl chain with α configuration showed the lowest values, being 2,6-dideoxy-L-*arabino*-hexopyranoside (**R3**) MIC = 25 μM and 2,6-dideoxy-D-*arabino*-hexopyranoside (**R7**) MIC = 50 μM. On the other hand, the corresponding β anomers (**R4** and **R8**, respectively) were inactive against the *Bacillus* species [8].

With respect to the 2-deoxy D-glycosides, both octyl and dodecyl β anomers showed MIC values equal to 112 μM and 93 μM, respectively, when tested against *E. faecalis*, being ineffective against the *Bacillus* species [7,8].

Despite the promising antibacterial activity of the tested compounds, all of them induced toxicity effects in peripheral blood human lymphocytes [8]. Hence, the next step in the investigation course was not only to improve the potency of the analogues but also to lower its toxicity.

In 2018, Rauter *et. al.* published a small library of new glycosides bearing a dodecyl chain. *O*-glycosides, *C*-glycosides and *S*-glycosides were synthesized, with varying deoxygenation patterns, sugar configuration, anomeric configuration and hexopyranoside vs. pentopyranoside structure (see Figure 1.12) [9,10].

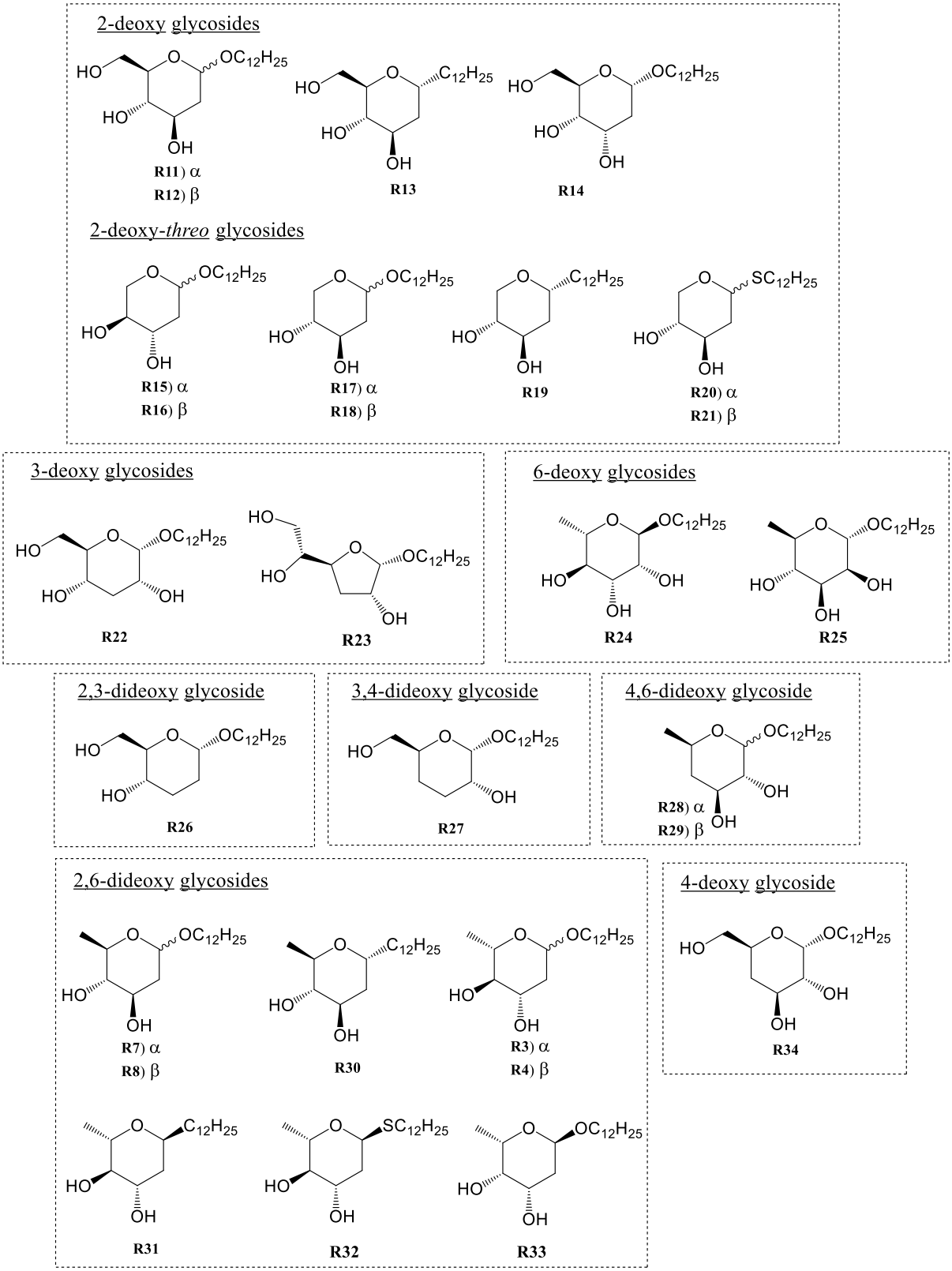

Figure 1.12. Deoxyglycosylation pattern of the synthesized compounds by Rauter et. al., bearing a dodecyl chain in the anomeric position [6–10].

2-deoxy *O*- and *S*-glycosides [9] were synthesized by a proven method where glycals react with a nucleophile in the presence of triphenylphosphane hydrobromide (TPHB) as catalyst [45]. This specific catalyst is used in order to minimize the formation of side products resulting from the Ferrier

rearrangement (common in acetal protected sugars), namely, the corresponding 3-deoxy sugar derivatives (see Scheme 1.3) [45,46]. The naturally occurring L-rhamnose, L-fucose, L-xylose and D-xylose were used as precursors for the glycal synthesis (see Scheme 1.4). In turn, reaction of the glycals with dodecan-1-ol, octan-1-ol or dodecan-1-thiol afforded the desired 2,6-dideoxy L-glycosides (**R3**, **R4**, **R32** and **R33**) and 2-deoxy-*threo* glycosides from the L- and D- series (**R15**, **R16** and **R17**, **R18**, **R20**, **R21**, respectively).

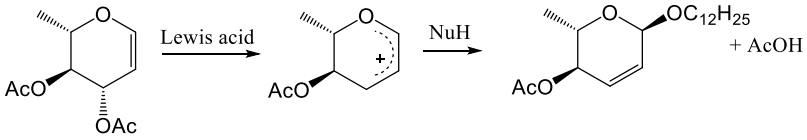

*Scheme 1.3. Ferrier rearrangement exemplified with compound **R3** [46].*

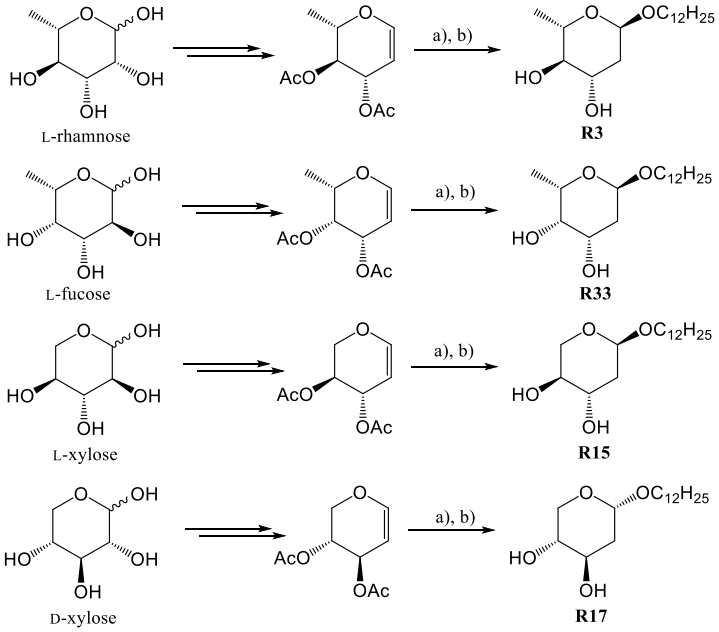

*Scheme 1.4. Synthesis of 2,6-dideoxy L-glycosides, exemplified with **R3** and **R33** and 2-deoxy-*threo *glycosides from the L- and D- series, exemplified with **R15** and **R17**, respectively. Reagents and conditions: a) dodecan-1-ol, TPHB, DCM, b) NaOMe, MeOH.*

In order to afford the 2,6-dideoxy D-glycosides (**R7** and **R8**), Rauter *et. al.* performed a deoxygenation reaction in position 6 in the respective 2-deoxy glycosides. It was accomplished by a tosylation reaction with tosyl chloride in pyridine and DCM followed by reduction with $LiAlH_4$ (see Scheme 1.5) [8].

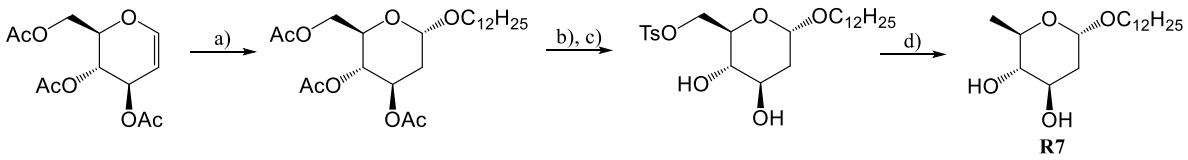

*Scheme 1.5. Route towards 2,6-dideoxy glycosylation followed by Rauter et. al. exemplified to synthesise compound **R7**. Reagents and conditions: a) dodecan-1-ol, TPHB, DCM, 83%; b) MeONa, MeOH, 95%; c) TsCl, DCM/Py, 93%; d) $LiAlH_4$, THF, 79% [8].*

Likewise, 6-deoxy glycosylation can also be achieved by the iodination of C-6 followed by reduction with $LiAlH_4$. This method was applied to afford **R25** with 66% yield over two steps [9].

The synthesis of the 3-deoxy glycoside **R22** could be achieved by taking advantage of the formation of the Ferrier rearrangement product, when using a glycal as substrate for the reaction. In this case, the glycoside was selectively oxidized in order to introduce an epoxide group at positions 2 and 3, which was then selectively reduced with $LiAlH_4$, as depicted in Scheme 1.6 [10].

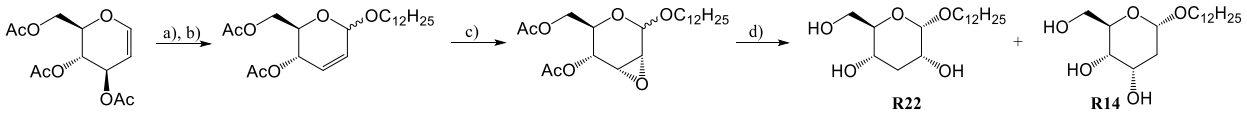

*Scheme 1.6. Synthesis of dodecyl 3-deoxy-α-D-ribo-hexopyranoside and 2-deoxy-α-D-ribo-hexopyranoside via epoxide[10]. Reagents and conditions:a) dodecan-1-ol, $BF_3{\cdot}Et_2O$; b)NaOMe, MeOH, (**α**, 73% over two steps and **β** 11% over two steps); c)m-CPBA, $NaHCO_3$, DCM, 74%; d)$LiAlH_4$, THF, (**R22**, 20% and **R14**, 33%)*

Another method followed to obtain 3-deoxy glycosides was the selective protection/deprotection strategy of a *ribo*-hexofuranoside, where positions 4 and 6 and 1 and 2 were protected with isopropilidene groups, leaving a free OH group in position 3. The OH in position 3 was triflated and reduced with *n*-Bu_4NBH_4 to afford the 3-deoxy pentopyranoside **R23** as major product and the analogous hexopyranoside **R22** as a minor product (see Scheme 1.7). This strategy allowed the team to have insights on the impact of the furanose ring on the antimicrobial activity over the pyranose ring [10].

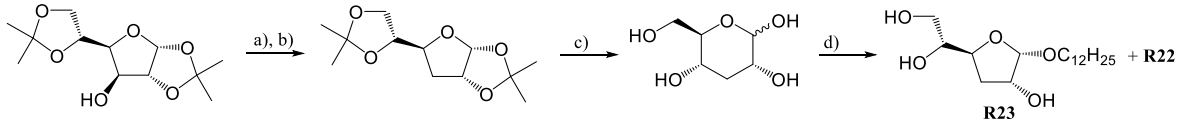

*Scheme 1.7. Synthesis of dodecyl 3-deoxy-α-D-ribo-hexopyranoside and -hexofuranoside, via Fisher glycosylation. Reagents and conditions: a) Tf_2O, py, DCM; b) n-Bu_4NBH_4, THF, 72% (over two steps); c) TFA, 90%; d) dodecan-1-ol, Amberlyst 15, (**R23**, 28% and **R22**, 8%) [10].*

In order to deoxygenate both 2 and 3 positions at the same time, Rauter *et. al.* performed a hydrogenation reaction of the benzyl protected Ferrier product to afford **R26** as depicted in Scheme 1.8 [10].

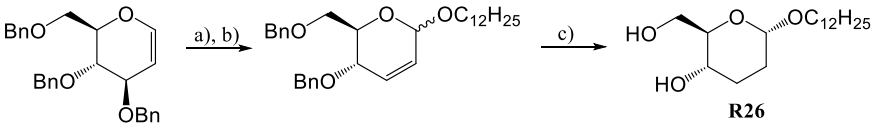

*Scheme 1.8. Synthesis of dodecyl 2,3-dideoxy-D-erythro-hexopyranoside **R26**. Reagents and conditions: a) dodecan-1-ol, HY, DCE, 43%; b) Et_3SiH 10 % Pd/C, 51%. HY refers to a specific zeolite and DCE to 1,2-dichloroethane [10].*

In the case of the 3,4-dideoxy glycoside, it was achieved by the selective protection of methyl α-D-glucose both 2 and 6 positions with a pivaloyl protecting group. The remaining free positions were triflated with triflic anhydride and reduced with tetrabutylammonium borohydride to afford the desired deoxy pattern. The selective protection of free sugars with pivaloyl esters have been described elsewhere [47].

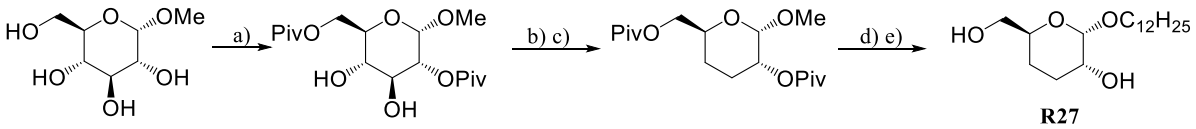

*Scheme 1.9. Synthesis of the 3,4-dideoxy glycoside **R21**. Reagents and conditions: PivCl, py, DCM, 65%; b) Tf_2O, py, DCM; c) n-Bu_4NBH_4, THF, 29% (over two steps); d) dodecan-1-ol, Amberlyst 15; d) KOH, H_2O/MeOH, 36% (over two steps).*

In order to access the 4-deoxy and 4,6-dideoxy pattern, the team proceeded with the regioselective protection of both 4 and 6 positions of methyl α-D-glucopyranoside with an acetal protecting group, followed by benzylation of the remaining free positions of the sugar. The regioselective opening of the benzylidene group with sodium cyanoborohydride afforded an intermediate compound with an OH group in position 4 and a benzyl group in position 6. Deoxygenation of C-4 was accomplished by triflation of position 4 followed by its reduction. In order to achieve the 4-deoxy glycoside **R34**, the co-workers introduced the dodecyl chain in C-1 and proceeded with the hydrogenation of the benzyl protecting groups. After isolating both anomers, the team selectively introduced a triflate group in the primary position of the sugar and reduced it with lithium aluminium hydride, affording the 4,6-dideoxy *O*-glycosides **R28** and **R29** (see Scheme 1.10) [9].

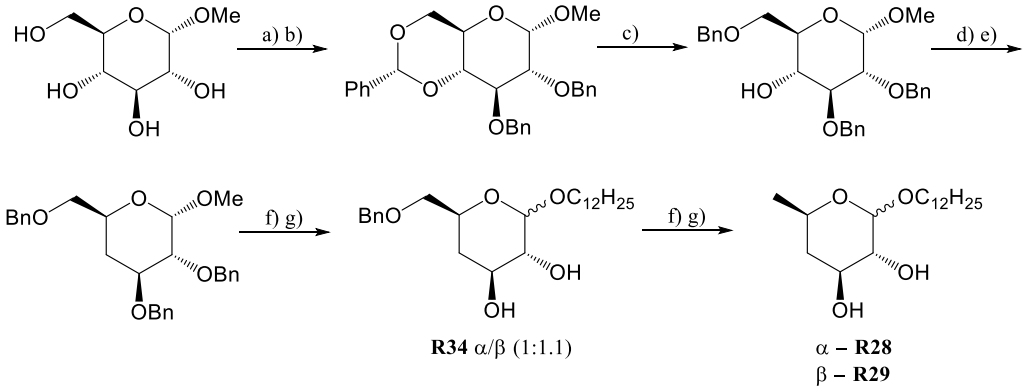

*Scheme 1.10. Synthetic route adopted by Rauter et. al. to afford the dodecyl 4-deoxy O-glycosides **R34** and the dodecyl 4,6-dideoxy O-glycosides **R29**. Reagents and conditions: a) $PhCH(OMe)_2$, p-TSA, DMF, 94%; b) BnBr, NaH, DMF, 82%; c)$NaBH_3CN$, I_2, ACN, 77%; d) Tf_2O, py, DCM; e) n-Bu_4NBH_4, THF, 83% (over two steps); f) dodecan-1-ol, Amberlyst 15; g) Et_3SiH, Pd/C, EtOAc, 80% (over two steps); h) Tf_2O, py, DCM; i) $LiAlH_4$, THF; g) Ac_2O, py, DMAP, 41% (over three steps); j) NaOMe, MeOH, 94-96% [9].*

C-glycosylation was assessed by an allylation reaction of the acetyl protected substrates followed by a metathesis reaction with undecene and a Grubbs type catalyst, to introduce the dodecyl chain in the molecule (see Scheme 1.11). The *C*-glycosides **R13**, **R14**, **R30** and **R31** were obtained by using its analogous deoxy *O*-glycosides acetylated in C-1 [9].

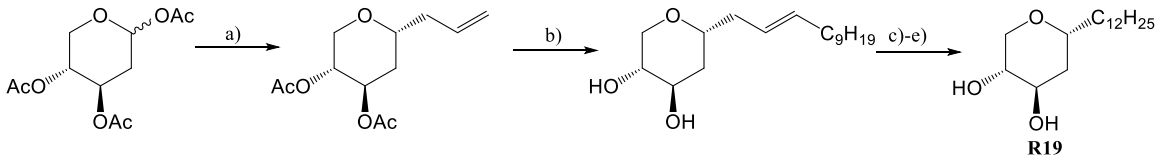

*Scheme 1.11. Methodology adopted by Rauter et.al. to access the C-glycosides using the corresponding O-glycosides as substrate. Here exemplified for **R19**. Reagents and conditions: a) $H_2C=CHCH_2Si(CH_3)_3$, $BF_3{\cdot}Et_2O$, ACN, 61%; b) undec-1-ene, 2nd generation Hoveyda-Grubbs catalyst; c)H_2, Pd/C, EtOAc; d) NaOMe, MeOH, 74% (over 3 steps) [9].*

The antimicrobial activity of the compounds described was assessed in *B. cereus*, *E. faecalis* and *B. anthracis* strains (sterne, pathonegic and ovine) (see [9,10] for more detailed information). The cytotoxicity was also assessed on Caco-2 cells and Hep G2 cells.

It was found out that 6-deoxy, 2,6-dideoxy and 4,6-dideoxy hexopyranosides were the most active ones (the α analogues showed MIC values between 12.6 μM and 56 μM). 4,6-dideoxy α-*O*-glycoside **R28** was the most promising compound, with MIC = 12.65 μM against all bacteria tested, accounting for half of the MIC value of the control against *B. anthracis* strains (chloramphenicol, MIC = 25 μM). In terms of cytotoxicity, the less toxic compounds were the *C*-glycosides, with IC_{50} >100 μM on Caco-cells. **R28** showed IC_{50} = 50 μM over Caco-cells and IC_{50} >100 μM over Hep G2 cells, although demonstrating the highest selectivity of bacteria *versus* eukaryotic cells [9,10].

On the structure-activity relationship, it was reported that the α configuration was essential for a good bioactivity, as well as the 6-deoxy pattern was crucial for effectiveness over *B. cereus* and *B. anthracis* Sterne. Also, the C-C linkage not only seemed to benefit D-series bioactivity but also to diminish the compounds cytotoxicity. On the other hand, C-3 and C-4 configuration does not appear to have any impact on the potency of the compounds. Finally, the furanose form revealed to be less potent when compared to the rest of the α-hexopyranosides, although it revealed IC_{50} = 100 μM [9,10].

The mechanism of action of the synthesized compounds was also investigated and it was proposed the carbohydrate – phospholipid interactions to be responsible for the bactericidal activity. It was, in fact, demonstrated that these deoxy glycosides' interactions caused phosphatidylethanolamine (PE) lamellar-to-inverted hexagonal phase transition, leading to envelope disruption and bacteria cell death in 10 min. The selectivity of these glycosides of bacteria cells over eukaryotic cells is explained by the fact that PE is abundant in the bacteria cell envelope whereas it is not in animal cells [9].

The fact that it was not observed the tendency to *B. anthracis* pore formation as well as any resistance mechanism to these deoxy compounds was also an advantage [9].

2 Objectives

Based on the excellent antibacterial properties exhibited by the 4,6-dideoxy α-*O*-glycoside **R28,** synthesized by Rauter *et. al*, the main goal of the presenting dissertation is to obtain the 4,6-dideoxy α-*C*-glycoside analogue for further evaluation, aiming to achieving bioactivity towards *B. anthracis* while minimizing compound's cytotoxicity.

To attain this purpose, the exploitation of an efficient synthetic route towards the desired *C*-glycoside is the major goal. Different starting materials and protection and deprotection methodologies are investigated along this work. Within the synthetic objectives, the first challenge is to obtain the 4,6-dideoxygenated pattern of the target structure, which will be accomplished with the exploration of protection/deprotection strategies in the sugar moiety. The second goal involves the *C*-glycosylation of the dideoxy framework to get the corresponding *C*-glycoside with α configuration. This constitutes a crucial synthetic objective in order to obtain the surfactant mimetic compound. See Scheme 2.1 for reactional steps elucidation.

Structural characterization of intermediates involved in the synthetic pathways and the final compound is also a main objective of this work. Deoxygenation pattern, C-C linkage formation, stereogenic center configuration and conformation of the synthesized compounds will be evaluated by 1D and 2D NMR spectra.

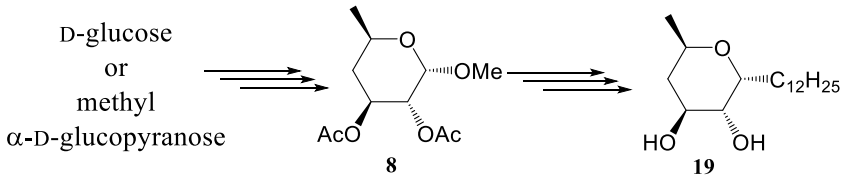

Scheme 2.1. General scheme of the steps pursued from two different starting materials in the development of the synthetic route towards the dodecyl 4,6-dideoxy glycoside.

.

3 Synthesis of a *C*-glycoside with a 4,6-dideoxygenation pattern and potential antimicrobial activity

3.1 Introduction

3.1.1 4,6-dideoxy glycosylation methods

Several mono deoxygenated sugars occur in the nature, such as 6-deoxy-L-mannose (L-rhamnose) and 6-deoxy-L-galactose (L-fucose), already mentioned in the text. One of the most important deoxy sugars in animal life is 2-deoxy-D-ribose, the monosaccharide present in the deoxyribonucleic acid (DNA). On the other hand, the only 3-deoxy sugar isolated from natural source is an adenine nucleoside isolated from the species *Cordyceps*, 3-deoxy-D-*erythro*-pentose. 4-deoxy glycosides haven been reported as non-existent in nature, however, it has been identified as a constituent in a lipopolysaccharide of *Citrobacter* specific strain (*Citrobacter braakii* PCM 1531) [48].

As for dideoxy sugars, 2,3-, 2,4- and 3,4-dideoxy sugars have not been found in nature. In the case of the 2,6-dideoxyhexoses, all of its diastereoisomers have been found in biologically active natural products, in some cases linked to flavone type compounds, such as D-oliose (2,6-dideoxy-D-*lyxo*-hexose), D-boivinose (2,6-dideoxy-D-*xylo*-hexose) and D-olivose (2,6-dideoxy-D-*arabino*-hexose), isolated from *Rhamnella inaequilatera* leaves (see [48] for more insight). 3,6-dideoxy monosaccharides, for instance, have been extensively studied in lipopolysaccharides of Gram (-) bacteria – abequose (3,6-dideoxy-D-*xylo*-hexopyranose), ascarylose (3,6-dideoxy-L-*arabino*-hexopyranose), colitose (3,6-dideoxy-L-*xylo*-hexopyranose). Curiously, antibodies induced by the vaccine conjugate against Gram (-) bacteria are quite always directed to target this particular dideoxy hexoses. In turn, 4,6-dideoxy sugars rarely occur in nature. Chalcose (4,6-dideoxy-3-*O*-methyl-D-*xylo*-hexopyranose), depicted in Figure 3.1, is a 4,6 dideoxy sugar isolated from chalcomycins or lankamycin (two types of macrolide antibiotics produced by *Streptomyces* sp.). 4,6-dideoxy-D-*xylo*-hexose (see Figure 3.1) is another 4,6-dideoxy analogue found in a macrolide isolated from *S. luteoverticillatus*. Finally, another naturally occurring 4,6-dideoxy glycoside is desosamine (4,6-dideoxy-3-dimethylamino-D-*xylo*-hexopyranose), depicted in Figure 3.1, found in the macrolide mycinamicin I [48].

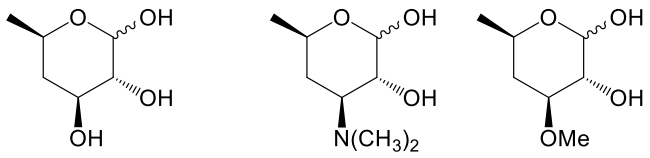

4,6-dideoxy-D-*xylo*-hexopyranose desosamine D-chalcose

Figure 3.1. Structure of the naturally occurring 4,6-dideoxy glycosides, D-chalcose, 4,6-dideoxy--xylo-hexopyranose and desosamine.

On the synthesis of these 4,6-dideoxy compounds, it has been described the use of the conventional protection/deprotection strategies. Starting from the partially deoxygenated L-rhamnosyl derivative protected with a 2,3-*O*-isopropilidene group, the Barton and McCombie procedure application afforded the deoxygenation in position 4, consequently achieving the 4,6-dideoxy pattern (see Scheme 3.1)[48,49]. A Barton McCombie type reaction is a two-step radical reaction where a secondary alcohol is replaced by a hydrogen atom, enabling the deoxygenation of a sugar's secondary positions. Usually, the first step comprises the conversion of the alcohol group in an *O*-thiocarbonyl group, while the second step is the radical reaction that replaces the *O*-thiocarbonyl group by a hydrogen [50].

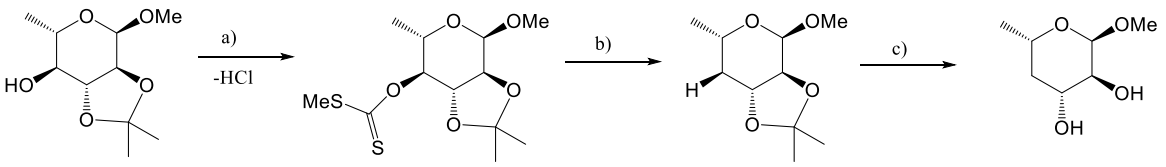

Scheme 3.1. Deoxygenation of secondary alcohols, where Pozsgay et al. deoxygenated C-4 by applying the Barton McCombie procedure. Reagents and conditions: a) NaH, im, CS_2, MeI, THF, 90% yield; b) Bu_3SnH, AIBN, 70% yield; c) TFA, 60% yield[49,50].

It has been reported the iodination of both 4 and 6 positions of a methyl glucopyranoside followed by its catalytic hydrogenation to achieve the required dideoxy patter, as depicted in Scheme 3.2 [48,51]. Wessel *et. al.* have also reported the formation of the diiodo glycoside, however they performed the reduction reaction with Bu_3SnH/AIBN [52,53].

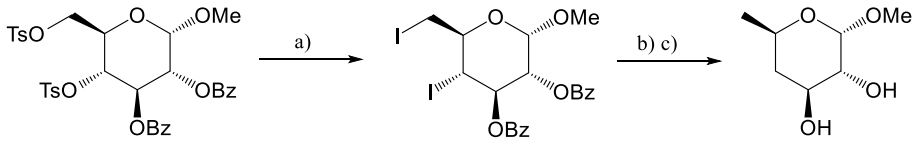

Scheme 3.2. Methodology used by to Siewert et.al in order to afford 4,6-dideoxy glycosylation. Reagents and conditions: a) NaI, DMF, 79%; b) H_2, Pd, 75%; c) NaOMe, MeOH [51].

The chlorination of positions 4 and 6 by the Jennings Jones method have also been described. Selective chlorination of positions 4 and 6 of methyl α-D-glucose with sulfuryl chloride was achieved followed by reduction of both halides with Bu_3SnH/AIBN, affording the 4,6-dideoxy glycon as depicted in Scheme 3.3 [48,54,55].

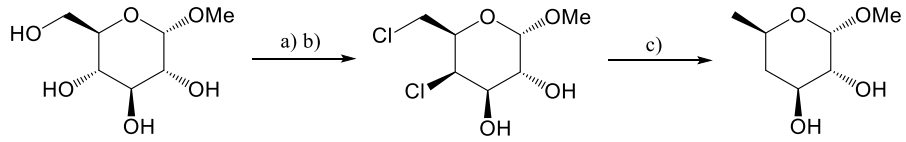

Scheme 3.3. Jennings Jones method to afford the 4,6-dideoxy pattern in methyl α-D-glucose. Reagents and conditions: a) SO_2Cl_2, py, $CHCl_3$; b) NaI, MeOH-H_2O, 50% (over two steps); c) Bu_3SnH, AIBN, toluene, 70%.

Despite these protection/deprotection methods of sugar moieties in order to obtain 4,6-dideoxy glycosylation, methodologies based on the cyclization of diene derivatives have been reported. For instance, D-chalcose has been synthesized by a cyclocondensation reaction a silyloxy diene with acetaldehyede in the presence of $Bf_3{\cdot}Et_2O$, as depicted in Scheme 3.4 [48,56].

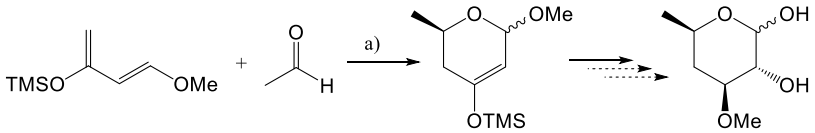

Scheme 3.4. Synthesis of D-chalcose through a cyclization strategy, by reaction of a silyloxy diene with acetaldehyde. Reagents and conditions:a) $Bf_3{\cdot}Et_2O$, 89% [48,56].

More recently, Sun *et.al.* proposed another example of a synthetic methodology towards D-chalcose by using acyclic reagents. They have synthesized D-chalcose and its C-3 epimer by using ethyl (*R*)-3-hydroxybutyrate (**I**) as starting material (see Scheme 3.5). The first step comprised the protection of the free OH group with a bulky silyl group, while the second consisted in the reduction of the ester functionality to an ether by Dibal-H, affording an aldehyde functionality in the structure (**II**). Reaction

with vinylmagnesium bromide, a Grignard reagent, originated the third intermediate compound (**III**) depicted in Scheme 3.5, which was methylated in the next reactional step (**IV**). Further reaction with a mixture of *t*-BuOH/H_2O in the presence of a specific osmium catalyst used in asymmetric synthesis, AD-mix-β [57], afforded the diol intermediate (**V**). Protection of both free alcohols with -OTBS groups followed by selective deprotection of the primary position with camphorsulfonic acid (CSA) made it possible to further oxidize the alcohol to aldehyde (by reaction with Dess-Martin periodinane). Posterior deprotection of the secondary -OTBS group with TBAF afforded **VI** which exists in equilibrium with its 4,6-dideoxy cyclic form[58].

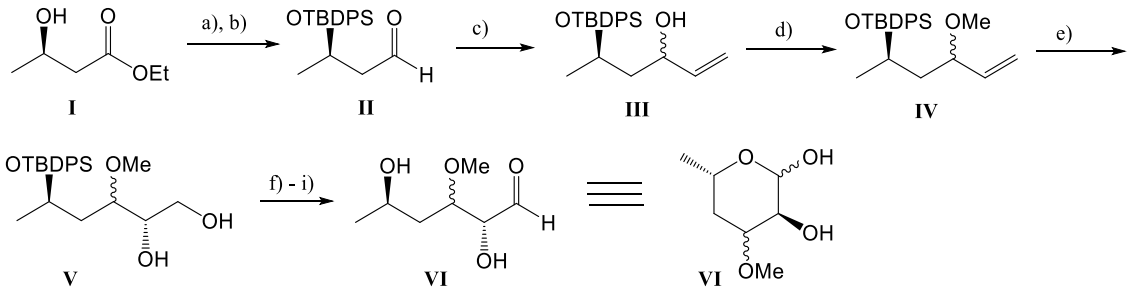

Scheme 3.5. Strategy employed by the authors to afford D-chalcose and its epimer in C-3, using acyclic intermediates. Reagents and conditions: a) TBDPSCl, DMAP, im, DCM, 99%; b) Dibal-H, DCM, 93%; c) vinylmagnesium bromide, CuI, Et_2O, 85%; d) MeI, t-BuOK, KOH, 96%; e) AD-mix-β, t-BuOH/H_2O, 82%; f)TBSOTf, 2,6-lutidine, DCM, 91%; g) CSA, MeOH, 60%; h) Dess-Martin periodinane, DCM, 86%, i) TBAF, THF, 83%. Note that AD-mix-β refers to a specific catalyst used in asymmetric synthesis [58].

3.1.2 *C*-glycosylation methods

C-glycosylation occurs when a new carbon-carbon bond is formed after reaction at the anomeric centre of the sugar. It has been subject of interest due to the occurrence of *C*-glycosyl compounds in glycolipids, oligosaccharides, glycoproteins and natural compounds [59]. Compared to the analogous *O*-glycosides, the *C*-glycosides are more stable as than the analogous *O*- or even *S*-glycosides, as they are inert towards hydrolytic enzymes *in vivo*. Dapagliflozin, canagliflozin and empagliflozin (compounds used against type II diabetes, see Figure 3.2) are examples of biologically active compounds in which the C-O glycosidic bond has been replaced by a C-C glycosidic bond in order to synthesize metabolically stable species [60]. On the naturally occurring *C*-glycosides, for instance, flavonoids are a class of compounds studied by our research group towards the Alzheimer disease [61–63], that have been reported to exhibit antibacterial activity [61,63–65].

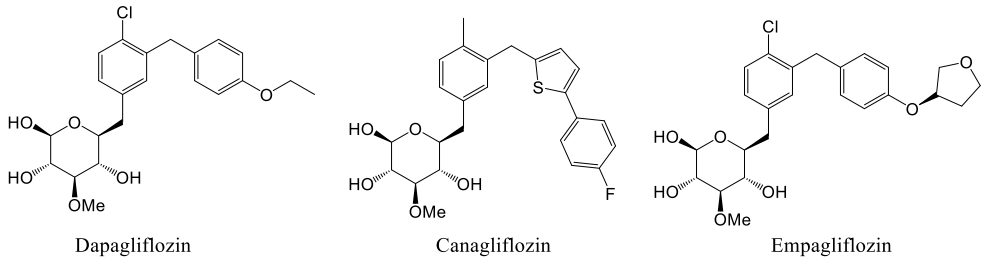

Figure 3.2. Structures of dapagliflozin, canagliflozin and empagliflozin.

The glycosyl donors may be methyl glycosides, glycals, glycosyl halides or acetates, 1,2-anhydro sugars, lactols or lactones, glycosyl imidates or phosphates or thioglycosides, sulfoxides or sulfones, and they can undergo an electrophilic/nucleophilic attack, radical fragmentation, formation of transition

metal complexes or rearrangements. Also, the precursors may be acyclic structures that later cyclize to give the desired sugar *C*-glycoside [60]. Yang *et. al.* reviewed all of the *C*-glycosylation methods used between the years 2000 and 2016 [60]. On the biologically active compounds, Liao *et. al.* have reviewed the *C*-glycosylation methods employed between the years 2007 and 2017 [66].

Carbohydrates with electrophilic character usually undergo reactions with nucleophilic carbons, where both α and β anomers are synthesized in different ratios. Glycosyl halides, -esters and -ethers are frequently used as glycosyl donors in *C*-glycosylation reactions, which can undergo a S_N2 or S_N1 pathway. In the case of S_N1 reactions, where there is formation of the oxocarbenium cation, the stereochemistry is generally controlled by hinderance effects. It is very common the use of zinc reagents (R-Zn), organolithium/aluminium (R-Li, R-Al) or Grignard (R-MgBr) derivatives as nucleophiles. Although they are effective, the reactional mixtures are air and moisture sensitive, thus difficult to manage [66]. Cyanides have also been used as nucleophiles - it has been reported the use of KCN as nucleophile, to give the cyano-derivative in 39% yield, as exemplified in Scheme 3.6 [60,67].

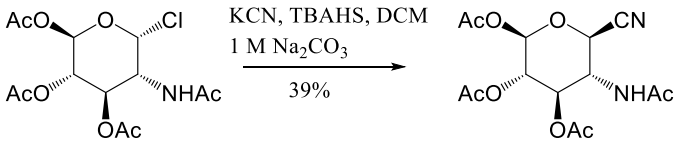

Scheme 3.6. Synthesis of a C-glycoside by reaction of a halide glycosyl donor and KCN in the presence of TBAHS as catalyst [60,67]. TBAHS refers to tetrabutylammonium hydrogen sulphate.

There was development of the *C*-glycosylation methods in order to carry out the reactions in milder conditions while being also effective. For example, the Fries type glycosylation or the palladium catalysed Heck-type *C*-glycosylation have been reported, where it is used Lewis acids/palladium complexes as reaction promoters[66].

A Fries type glycosylation generates a *C*-glycosylphenol through reaction of a glycosyl donor with a phenol in the presence of an activator. This one-pot reaction is useful in the synthesis of flavone derivatives and it involves a rearrangement of an *O*-glycoside to form the *C*-glycoside, as depicted in Scheme 3.7. TMSOTf and $BF_3{\cdot}Et_2O$ are examples of Lewis acids usually used as reaction promoters [68].

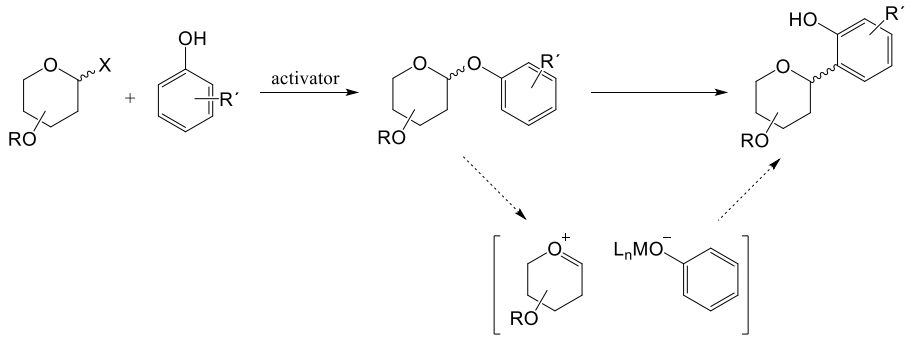

Scheme 3.7. Mechanism of the Fries-type rearrangement proposed by Rauter et. al. [68].

Glycosylation reactions involving glycals have already been mentioned in the previous section 1.2.4, where it was discussed the formation of *O*-glycosides (see reaction A, Scheme 3.8). In the case of the *C*-glycosides, carbon nucleophiles should be used as reagents. The Heck-type reaction is a less common *C*-glycosylation reaction, which involves the use of palladium, a transition metal. However it has de

advantage of being highly effective and with an improved stereocontrol over the products' configuration. Scheme 3.8, reactions A, B and C illustrate different possibilities of palladium catalysed *C*-glycosylations. In particular, a highly stereoselective palladium-catalysed decarboxylative glycosylation reaction was used by Liu *et. al.* in order to synthesize the macrolide aspergillide A with β configuration (Scheme 3.9), cytotoxic to leukemia cells [66,69].

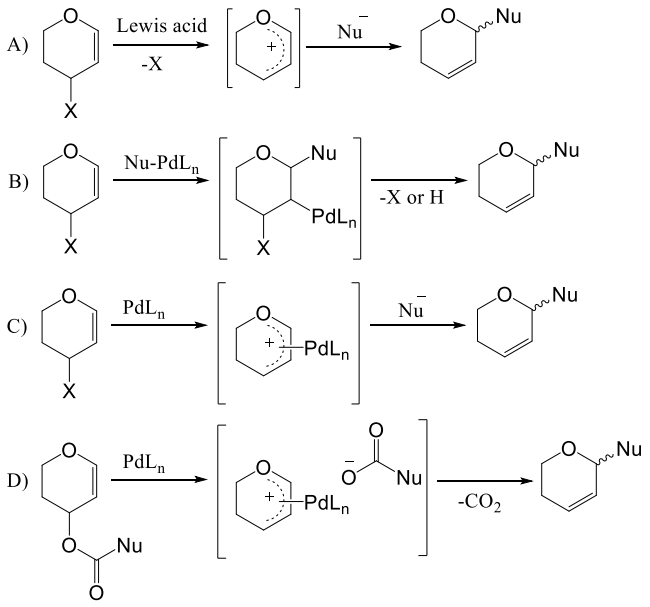

Scheme 3.8. General scheme of a typical glycosylation using a glycal as substrate in the presence of a Lewis acid as promoter (A) and palladium catalysts (B, C, D).

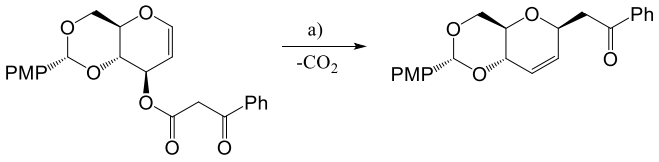

Scheme 3.9. Heck-type C-glycosylation reaction used by in the synthesis of the macrolide aspergillide A. Reagents and conditions: a) Pd(OAc)2, DiPPF, toluene, 88%. Note that DiPPF refers to 1,1'- bis(diisopropylphosphino)ferrocene [69].

Radical fragmentation reactions are also a possible *C*-glycosylation methodology. It is mostly documented to occur when the substrate reacts with Bu_3SnH in the presence of AIBN (2,2´-azobisisobutyronitrile) as radial initiator [60]. In Scheme 3.10 it is illustrated an example of a direct allylation of a glycosyl halide in the presence of allyltrimethylstannane in the presence of AIBN affording the α anomer as major product in 73% yield [70].

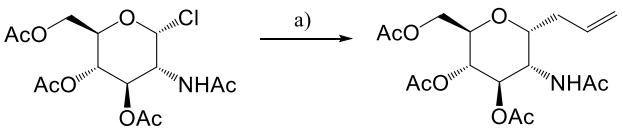

Scheme 3.10. Synthesis of an allyl glycoside through a radicalar reaction, using a glycosyl halide as substrate. Reagents and conditions: allyltrimethylstannane, AIBN, 73% [70].

Herbicidins are a class of nucleoside antibiotics used in plants against *Xanthoman oryzae*, also embody a *C*-glycosidic bond in its structure. Trauner *et. al*. reported the synthesis of the *C*-glycoside Herbicidin C through reaction of 1,6-anhydro D-glucose protected with benzyl groups in 2, 3 and 4 positions, with allyltrimethylsilane, catalysed by TMSOTf (see Scheme 3.11) [66,71].

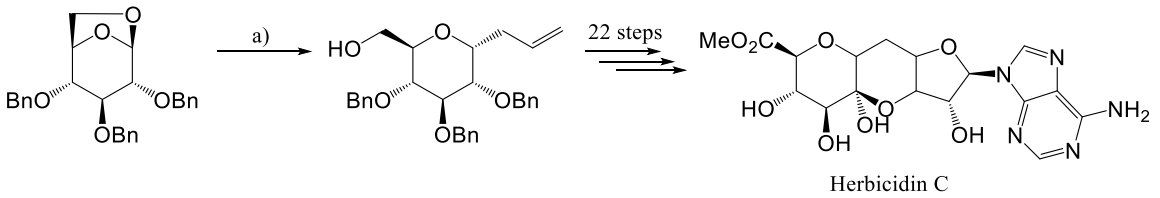

Scheme 3.11. C-glycosylation step carried out in the synthesis of Herbicidin C reported Trauner et. al. Reagents and conditions: a) allyltrimethylsilane, TMSOTf, 66% [66,71].

Pluramycins are aryl *C*-glycosides that besides showing antimicrobial activity also revealed to be active against tumors. Suzuki *et. al.* carried out the synthesis of pluramycin A, where the *C*-glycosylation reaction used the anomeric mixture of the acetyl glycoside as glycosyl donor. The reaction with the tricyclic aryl structure in the presence of $Sc(OTf)_3$ to afford the α-*C*-glycoside in 89% yield [66,72].

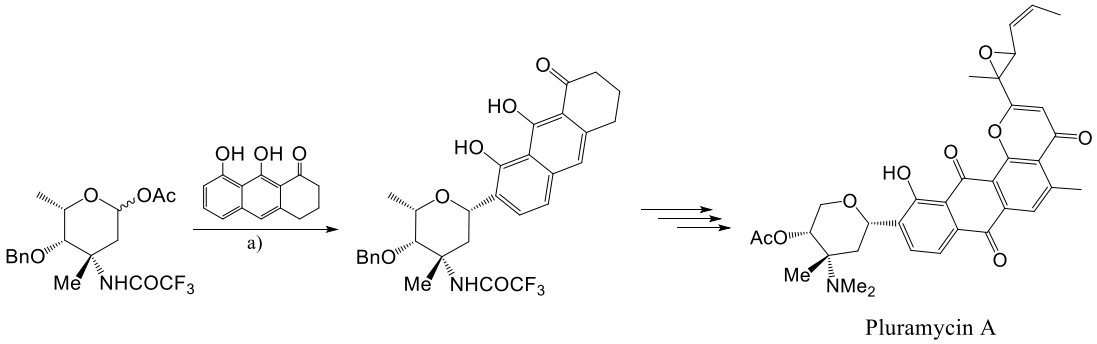

Scheme 3.12. C-glycosylation step carried out in the synthesis of Pluramycin A, reported Suzuki et. al. *Reagents and conditions: a) $Sc(OTf)_3$, drierite, DCE, 89% [66,72] .*

Since the mechanistic principles behind the *C*-glycosylation stereoselectivity is not fully disclosed, the search for stereoselective reactions continues to be a major challenge [60,66].

3.2 Results and Discussion

3.2.1 Synthetic routes

The purpose of this approach was to explore the capacity of benzoyl group at position 4 of D-glucose as leaving group towards a S_N2 reaction[80]. To do so, we selectively introduced an acetal protecting group at positions 4 and 6 of D-glucose – a benzylidene group, followed by benzylation of the remaining unprotected positions and finally, regioselective opening of the acetal group with iodosuccinimide (NIS), as depicted in Scheme 3.13.

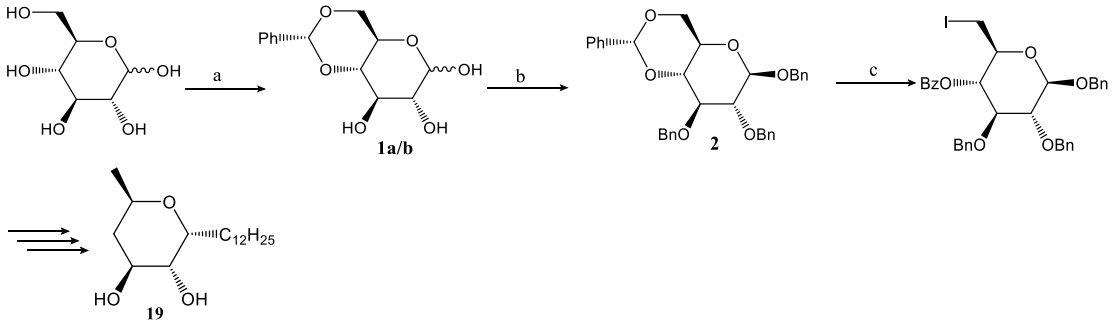

*Scheme 3.13. Synthetic route proposal for the synthesis of **19** using D-glucose as starting material. Reagents and conditions: a) $PhCH(OCH_3)_2$, p-TSA, DMF; b) BnBr, NaH, DMF, 6% over two steps; c) NIS, CCl_4, $BaCO_3$.*

The use of the benzylidene acetal as a protecting group is a very well-known strategy to selectively protect diols. In this case, the reaction was carried out by the addition of benzaldehyde dimethyl acetal to a solution of the commercial mixture of α- and β-D-glucose in DMF, in the presence of *p*-toluenesulfonic acid (*p*-TSA). As depicted in Scheme 3.14, it is necessary to use a Lewis acid as a catalyst to activate the methoxy groups in the benzaldehyde dimethyl acetal, in order to turn them into good leaving groups and consequently promote the nucleophilic attack by one of the free hydroxy groups. The mechanism is repeated once again with the other hydroxy group to form the cyclic acetal. The solvent choice must take in consideration that in a S_N2 reaction, the nucleophilic attack is easier if the nucleophile is not solvated. Therefore, it is important to use an aprotic solvent, such as DMF, as it will promote the existence of the nucleophile as a "naked anion", through the prevention of nucleophile-solvent hydrogen bond interactions.

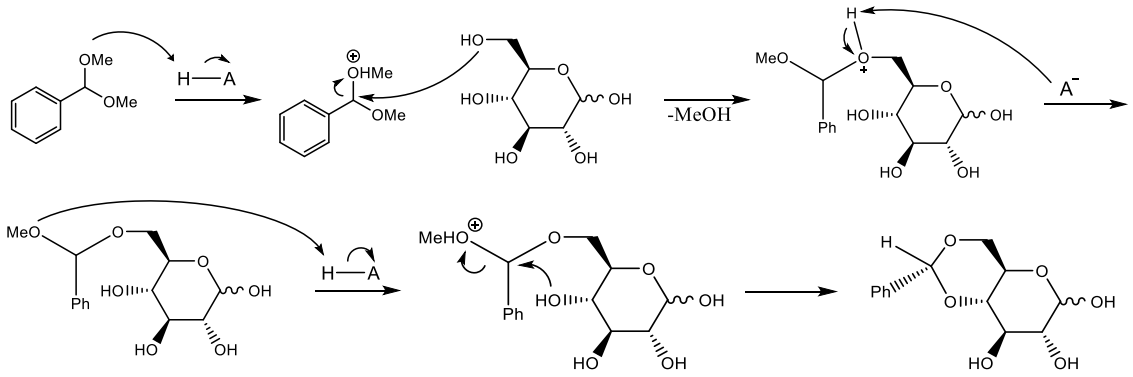

Scheme 3.14. Mechanism underlying the protection of positions 4 and 6 of D-glucose with a benzylidene acetal group, where HA refers to the Lewis acid used, in this case, p-TSA.

The reaction led to the anomeric mixture which could not be separated as carbon 1 belongs to a hemiacetal. By analysis of the ^{1}H NMR spectrum, it was possible to notice the appearance of two multiplets between δ 7.34 – δ 7.53 ppm (chemical shift characteristic of phenolic protons), integrating in ratio 2:3 protons, in accordance to the presence of a monosubstituted phenol compound. The aromatic ring is symmetric and thus one signal is assigned to protons 1 integrating 2H and the other signal comprises resonances of protons 2 and proton 3 integrating 3H (see Figure 3.3). Since we were in the presence of a mixture of two anomers, in proportion 1:1, the signals integrate to 4 and 6 protons. Also, in ^{13}C NMR spectrum, the corresponding carbon signals were duplicated.

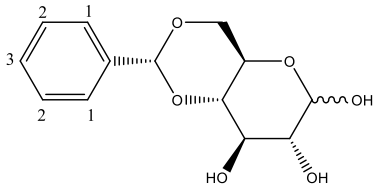

*Figure 3.3. Structure of compounds **1α/β** highlighting numbering of the aromatic protons.*

The spectrum also exhibits a broad singlet at δ 5.59 ppm, integrating 2H, a higher chemical shift than the expected for the anomeric proton. As these protons correlate with the aromatic carbons (correlation visible in HMBC), it can be confirmed that these signals correspond to the acetal proton H-7 of both anomers. Hence, it can be confirmed the presence of the benzylidene group in both α and β anomers. While H-7α/β belongs to an acetal function suffering also a deshielding effect caused by the neighbouring phenol group, H-1α/β belongs to a hemiacetal, appearing also at higher chemical shift than the remaining protons in the sugar moiety. Consequently, it is possible to identify the anomeric protons as doublets at δ 5.16 ppm and δ 4.62 ppm. By determining the coupling constants of both signals ($J_{1\beta,2\beta}$ = 7.88Hz, $J_{1\alpha,2\alpha}$ = 3.10Hz), it was possible to understand which signal corresponds to the α anomer and the β anomer, as the coupling constant between H-1α and H-2 is expectedly lower than the one between H-1β and H-2 due to the fact that H-1 β and H-2 were trans diaxial to each other, with a dihedral angle close to 180º (see Figure 1.4, section 1.1.3, page 5).

As it was impossible to purify the compounds, that, as hemiacetals, suffer from mutarotation as a result of the equilibrium through the acyclic form, the second step of the synthetic route – the benzylation reaction, was accomplished using the mixture of the anomers in a well-defined ratio (α:β, 1:1).

To benzilate the remaining free OH groups, sodium hydride was added to a solution of the anomeric mixture in DMF. Only after 15 minutes, benzyl bromide was added. The NaH plays an important role as it is a strong base and thus it can remove the proton from the OH groups generating anions, facilitating the nucleophilic attack to the benzyl bromide (see Scheme 3.15).

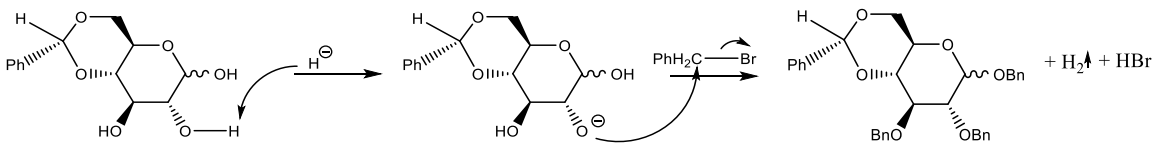

Scheme 3.15. Mechanism underlying the benzylation reaction.

After 3.5h, the TLC revealed the formation of two major products. In this case, the isolation of the anomers was possible, but the benzylated anomer was isolated only in 6% yield (yield calculated over two steps). When analysing the ^{1}H NMR spectrum, it was possible to confirm the presence of the benzyl groups since the integration of the aromatic proton's signals increased to 20, as well as there were three AB systems (between δ 5.01 ppm and δ 4.71 ppm), characteristic of the -CH_2 moiety in benzyl groups.

After protecting all the positions of the sugar, the next step was to regioselectively open the benzylidene group in order to obtain a benzoyl group at position 4 and position 6 protected with iodide. The main goal of this reaction was to investigate the reactivity of the position 4 of the sugar, through a S_N2 reaction with iodine, with the purpose of easily obtaining the desired 4,6-dideoxy sugar moiety by reduction over 2 reactional steps after the benzylidene opening reaction, as depicted in Scheme 3.16.

Since the yield of the benzylation reaction (see Scheme 3.13, step b) was very low, methyl 2,3-di-*O*-benzyl-4,6-*O*-benzylidene-α-D-glucopyranoside (**A**), already available in our laboratory, was used as starting material to be regioselectively opened with NIS (see Scheme 3.16).

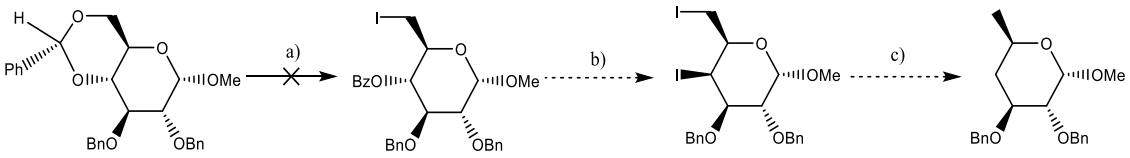

Scheme 3.16. Synthetic route initially designed to obtain the 4,6-dideoxy pattern in 5 reactional steps, starting from commercial D-glucose. Reagents and conditions: a) NIS, CCl_4, $BaCO_3$; b),LiI, 2,4,6-trimethilpyridine, py[87]; c) H_2, Pd/C, dipea, THF/MeOH.

Usually, this type of reaction is performed using NIS, $BaCO_3$ and CCl_4 as the solvent and, when needed, 1,1,2,2-carbon tetrachloride as a cosolvent. At the first attempt, the reaction was carried out using chloroform ($CHCl_3$) as solvent, leading to the formation of a complex mixture together with a high amount of the remaining starting material (Table 3.1, entry 1). The reaction was repeated in CCl_4, however, when following the reaction by TLC, the result was similar to the one of the previous attempt (Table 3.1, entry 2). The reaction was then repeated several times, in different conditions, as described in Table 3.1 (entries 1-4). Since the starting material did not react in an acceptable extent, the reaction was repeated using methyl 2,3-di-*O*-acetyl-4,6-*O*-benzylidene-α-D-glucopyranoside **4** (see Table 3.1, entry 5) and NBS instead of NIS. By TLC, it was possible to observe that the starting material reacted completely to give a new compound with lower polarity, in higher amount when compared to the side products also formed.

*Table 3.1. Reaction conditions to selectively open the benzylidene group. Compound **A** corresponds to methyl 2,3-di-O-benzyl-4,6-O-benzylidene-α-D-glucopyranoside, **4** corresponds to methyl 2,3-di-O-acetyl-4,6-O-benzylidene-α-D-glucopyranoside and **5** corresponds to methyl 2,3-di-O-acetyl-4-O-benzoyl-6-bromo-6-deoxy-α-D-glucopyranoside.*

Entry	Starting material[a]	Solvent	Reagents	Equivalents	Time	Temperature /ºC	Reaction outcome
1	**A**	$CHCl_3$	NIS	0.95	20h	Reflux	Complex mixture
			$BaCO_3$	0.95			
2	**A**	CCl_4	NIS	1.1	20h	Reflux	Complex mixture
			$BaCO_3$	1.1			
3	**A**	CCl_4	NIS	1.1	30min	66ºC	Complex mixture[b]
			$BaCO_3$	1.1			
4	**A**		NIS	0.95	24h	Reflux	

		CCl_4 + $CHCl_3$	$BaCO_3$	0.95			Complex mixture
5	**4**	CCl_4	NBS	1.2	2.5h	Reflux	Formation of **5** in 50% yield
			$BaCO_3$	2.7			

a) Compound **A** was available at the Carbohydrate Chemistry Laboratory and was not synthesized.
b) The reaction was carried out in a microwave reactor at 250Psi, 150W.

After purification, when comparing the resulting NMR spectrum of **5** with the starting material **4**, it was possible to observe that not only the singlet (δ 5.53 ppm) corresponding to the H-7 in the acetal protecting group disappeared, but the C-6 chemical shift decreased to δ 31.4 ppm, resulting from the shielding effect caused by the presence of the bromide group at the position 6 of the sugar. Also, there is a new quaternary carbon signal corresponding to the carbon present in the new carbonyl group. Hence, we were able to understand that the new compound was methyl 2,3-di-*O*-acetyl-4-*O*-benzoyl-6-bromo-α-D-glucopyranoside (**5**).

In fact, the presence of the benzyl protecting groups seems to be decisive for the reaction, as it did not occur with the benzylated sugar derivative. The mechanism underlying this type of benzylidene ring opening starts by the abstraction of the acidic proton in the acetal by the halide radical, provided by the *N*-bromosuccinimide. It is followed by the attack of another bromine radical to the least hindered position of the acetal, originating the sugar derivative with the halide in position 6 and the benzoyl group in position 4 (path 1, Scheme 3.17). Alternatively, it can undergo an ionic pathway, where there is the formation of an unstable bromoacetal which suffers fragmentation to a cyclic carbocation and a bromide, which in turn attacks the least hindered position of the acetal to give the desired product (path 2, Scheme 3.17) [81,82].

However, in this case, it seems that there is competition in the rate limiting step of the reaction (the abstraction of the benzylic proton), between the H-7 (acetal proton) and the benzyl ether protons [83,84], generating complex mixtures, consuming NBS that is only available to react with a small amount of starting material.

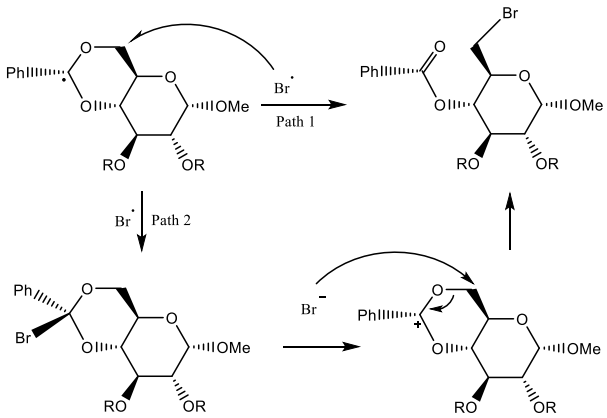

Scheme 3.17. Possible mechanisms of the oxidative fragmentation of benzylidene acetal [81,82].

Protection of the positions 2 and 3 of the sugar with acetate protecting groups was not compatible with the planned synthetic route, as both acetate and benzoyl groups are esters, and no selectivity is expected when performing the following S_N2 reaction. Therefore, this synthetic pathway was abandoned and synthetic route B adopted.

3.2.2 Other synthetic routes

After trying other synthetic routes, the intermediate methyl 4,6-dideoxyglycoside was obtained over 8 steps in 20% overall yield and the target *C*-glycoside in 13% overall yield starting from methyl α-D-glucopyranoside.

4 Conclusion

The main aim of the present dissertation was accomplished by the synthesis of the new dodecyl 4,6-dideoxy *C*-glycoside **19**. The first approach was made through a synthetic route starting from the naturally occurring D-glucose. Regioselective protection of both 4 and 6 positions followed by benzylation of the remaining free positions was achieved with 6% yield over the two steps. The regioselective opening of the benzylidene group with *N*-iodosuccinimide was not successful may be due to competition reactions with the benzyl protecting groups in C-2 and C-3. Alternatively, synthetic routes were tried, using methyl α-D-glucoside as starting material. After several protection/deprotection strategies, dodecyl 4,6-dideoxy-α-D-hexopyranoside **19** was synthesized in 13% yield over 13 synthetic steps.

When compared to the analogue *O*-glycoside **R28** synthesized by Rauter *et. al.* (15% yield over 11 steps), the yield was similar. Although achieved through less synthetic steps, the methodology used in this work in order to afford the *C*-glycoside was easier to carry out as the intermediate compounds were stable, as well as the hydrogenation reaction mixtures were easily purified through liquid-liquid extractions.

Concluding, it was afforded a new dodecyl 4,6-dideoxy glycoside with potential application as antimicrobial compound against *B. anthracis* with expected lower cytotoxicity than the analogue *O*-glycoside **R28**. Future biological assays will disclose these expectations.

5 Experimental

5.1 Instrumentation, reagents, solvents and purification techniques

The reagents used throughout the synthetic route were commercially acquired from Sigma-Aldrich, Fischer, Acros and Fluka, as well as the solvents (p.a. grade), with a purity grade prior to 98%, as mentioned in the label, and were not submitted to any purification before using. In some cases, the solvents were dried, prior to use, with activated molecular sieves 3Å. In order to weight the compounds, it was used an analytical digital scale from *KERN ALJ*, 220-4 model, with a $\pm 10^{-4}$g precision. When necessary, it was used an ultrasonic bath (VWR™ Ultrasonic Cleaner) to promote the compound's dissolution.

The reaction's progression was carried out via TLC plates (20 x 20 cm aluminium sheets coated with silica gel, Ref. 60 F_{254}, 0,2 mm thick, purchased from Merck) through UV light detection followed by revealing with a H_2SO_4/MeOH 10% (v/v) solution and heating up to 400ºC. The compounds were purified by column chromatography using silica gel (60, 0.040-0.063 mm, purchased from Merck) as the stationary phase and a mixture of the adequate solvents as the mobile phase.
The experimental characterization was accomplished through nuclear magnetic resonance (NMR) spectrum with a Bruker Advance 400 spectrometer at 25ºC, operating at 100.62 MHz for ^{13}C NMR and 400.13 MHz for ^{1}H NMR. $CDCl_3$ and CD_3OD (purchased from Sigma-Aldrich) were the solvents used to carry out the NMR analysis. The compounds were submitted to ^{1}H NMR, ^{13}C NMR, COSY, HMBC and HSQC experiments and the obtained results are expressed as chemical shifts (δ, reported in ppm) and coupling constants (*J*, reported in Hz). The spectra were analysed using either the TopSpin 3.0 or MestreNova software.
The optical rotations ($[\alpha]_D^{20.0}$) were obtained with a Perkin Elmer 343 polarimeter at 20ºC, with an optical percurs of 1cm, using solutions of 10 mg/mL (1c). The melting points were measured on a SMP 30 capillary apparatus (Stuart Scientific, Bibby).

5.2 Synthesis

5.2.1 Synthesis of 4,6-*O*-benzylidene-D-glucopyranose (**1a/b**).

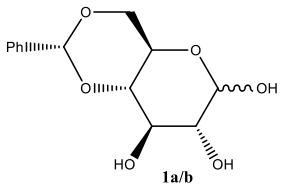

1a/b

A mixture of D-glucose (0.5 g, 2.78 mmol), benzaldehyde dimethyl acetal (0.46 g, 0.31 mmol), *p*-toluenesulfonic acid (0.96 mg, 0.006 mmol) in dry DMF (2 mL) was heated to 60 ºC in a vigorous stirring flask, while N_2 was being bubbled through the reaction mixture in order to ensure rapid removal of the forming MeOH. The reaction was followed by TLC using DCM/MeOH (12:1) as eluent and after 2.5 h, it was quenched by cooling and adding an excess of Et_3N. The solvent was evaporated under reduced pressure and it was obtained a syrup which was directly purified by chromatographic column using Hex/EtOAc (140:1) as eluent. The mixture of α and β anomers of compound **1a/b** (1.72 g) was obtained as white crystals in 1:1 ratio. M.p. = 178 ºC – 180 ºC; Rf = 0.35 DCM/MeOH (12:1); **^{1}H NMR** ($CDCl_3$, 400 MHz): δ 7.52 – 7.51 (m, 4H, H aromatic), 7.37 – 7.35 (m, 6H, H aromatic), 5.59 (s, 2H, H-7α, H-7β), 5.16 (br d, 1H, H-1α, $J_{1\alpha,2\alpha}$ = 3.10Hz), 4.62 (d, 1H, H-1β, $J_{1\beta,2\beta}$ = 7.88Hz), 4.28 (dd, 1H, H-6βa, $J_{6\beta a,6\beta b}$ = 10.62Hz, $J_{5\beta,6\beta a}$ = 4.31Hz), 4.20 (dd, 1H, H-6αa, $J_{6\alpha b,6\alpha a}$ = 10.11Hz, $J_{5\alpha,4\alpha}$ = 4.76Hz), 4.00 (dt, 1H, H-5α),3.89 (t, 1H, H-3α, $J_{3\alpha,4\alpha}$ = $J_{3\alpha,2\alpha}$ = 9.19Hz), 3.80 – 3.72 (m, 2H, H-6βb, H-6αb), 3.65 (t,

1H, H-3β, $J_{3\beta,4\beta}$ = 8.61Hz), 3.51 – 3.43 (m, 4H, H-4β, H-5β, H-2α, H-4α), 3.26 (dd, 1H, H-2β, $J_{2\beta,3\beta}$ = 8.19Hz). **^{13}C NMR** ($CDCl_3$, 400 MHz): δ 137.7 - 126.1 (C aromatic), 101.6, 101.5 (C-7α or C-7β), 97.6 (C-1β), 93.3 (C-1α), 81.8, 81.1 (C-4β or C-4α), 75.8 (C-2β), 73.3 (C-3β), 73.1 (C-2α), 70.4 (C-3α), 68.9 (C-6α), 68.4 (C-6β), 66.4 (C-5β), 62.1 (C-5α). Spectroscopic data are in agreement with the literature[85].

5.2.2 Synthesis of benzyl 2,3-di-*O*-benzyl-4,6-*O*-benzylidene-α-D-glucopyranoside (**2**).

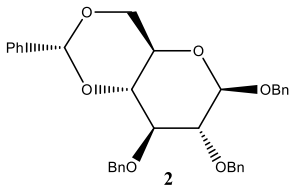

2

To a solution of **1a/b** (0.21 g, 0.45 mmol) in DMF (4 mL), sodium hydride (60% paraffin suspension, 0.38 g, 2.23 mmol) was carefully added at 0 ºC and the reaction was stirred for 15 min. Then, benzyl bromide (0.04 mL, 2.23 mmol) was added to the mixture and stirred at room temperature for 3.5 h, under nitrogen atmosphere. The reaction was quenched by pouring it into cooled water (100mL) and extracted with DCM (3 x 100 mL). The organic layers were combined, dried with $MgSO_4$, the solids were filtered off and the filtrate concentrated in vacuum. Purification was achieved by chromatographic column, using a gradient of Hex/EtOAc (25:1) → Hex/EtOAc (20:1) as eluent, affording the compound **2** (27.10 mg) as a syrup in 6% yield over two steps.$[\alpha]_D$ = -3.7 (*c* 1.0, $CHCl_3$); Rf = 0.66 Hex/EtOAc (3:1); **^{1}H NMR** ($CDCl_3$, 400 MHz): δ 7.55 – 7.28 (m, 20H, H aromatic), 5.63 (s, 1H, -OC<u>H</u>Ph), 5.02, 4.99 (Part A of AB system 1, 1H, -OC<u>H</u>$_2$Ph, J_{AB} = 11.86 Hz), 4.98, 4.95 (Part A of AB system 2, 1H, -OC<u>H</u>$_2$Ph, J_{AB} = 11.38Hz)*, 4.97, 4.94 (Part A of AB system 3, 1H, -OC<u>H</u>$_2$Ph, J_{AB} = 10.67Hz)*, 4.86, 4.83 (Part B of AB system 2, 1H, -OC<u>H</u>$_2$Ph)*, 4.84, 4.81 (Part B of AB system 3, 1H, -OC<u>H</u>$_2$Ph)*, 4.74, 4.71 (Part B of AB system 1, 1H, -OC<u>H</u>$_2$Ph), 4.69 (d, 1H, H-1, $J_{1,2}$ = 8.26Hz), 4.43 (dd, 1H, H-6a, $J_{6a,5}$ = 5.07 Hz, $J_{6a,6b}$ = 10.36Hz), 3.83 – 3.73 (m, H-3, H-4), 3.87 (t, 1H, H-6b, $J_{6b,5}$ = 10.19Hz), 3.59 (t, 1H, H-2, $J_{2,3}$ = 8.52Hz), 3.48 (td, H-5, $J_{5,4}$ = 9.68Hz). **^{13}C NMR** ($CDCl_3$, 400 MHz): δ 138.5, 138.3, 137.3, 137.1 (Cq aromatic), 129.0 – 126.1 (C aromatic), 103.1 (C-1), 101.2 (-O<u>C</u>HPh), 82.2 (C-2), 81.5 (C-3 or C-4), 81.0 (C-4 or C-3), 75.5 (-O<u>C</u>H$_2$Ph – 3)*, 75.2 (O<u>C</u>H$_2$Ph – 2)*, 71.6 (O<u>C</u>H$_2$Ph – 1), 68.9 (C-6), 66.1 (C-5).

* permutable

5.2.3 Synthesis of methyl 4,6-*O*-benzylidene-α-D-glucopyranoside (**3**)

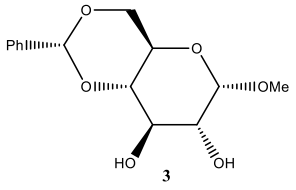

3

The mixture of methyl α-D-glucopyranoside (5.00 g, 25.74 mmol), benzaldehyde dimethyl acetal (7.84 g, 51.50 mmol), *p*-toluenesulfonic acid (0.047g, 0.30 mmol) in dry DMF (25 mL) was heated to 60 ºC under a pressure of 240 mbar, in order to continuously remove the MeOH from the reaction mixture. The reaction was followed by TLC using Hex/EtOAc (1:3) for 2 h. After total consumption of the starting material, the mixture was cooled and extracted with DCM (2 x 300 mL) and water (200 mL). The organic layers were combined, dried with $MgSO_4$, the solids were filtered off and the filtrate

concentrated in vacuum. Purification was achieved by recrystallization with isopropanol. Compound **3** (6.54 g) was obtained as white crystals in 90% yield. M.p = 166 ºC - 169 ºC; Rf = 0.22 Hex/EtOAc (1:3); **^{1}H NMR** ($CDCl_3$, 400 MHz): δ 7.53 – 7.50 (m, 2H, H-aromatic), 7.41 – 7.38 (m, 3H, H-aromatic), 5.56 (s, 1H, H-7), 4.83 (d, 1H, H-1, $J_{1,2}$ = 3.76Hz), 4.32 (dd, 1H, H-6a, $J_{6a,6b}$ = 9.55Hz, $J_{6a,5}$ = 4.35Hz), 3.97 (t, 1H, H-3, $J_{3,4}$ = $J_{2,3}$ = 9.32Hz), 3.87 – 3.85 (m, 2H, H-5, H-6b), 3.67 (dd, 1H, H-2), 3.53 (t, 1H, H-4, $J_{4,5}$ = $J_{3,4}$ = 9.32Hz), 3.49 (s, 3H, -OC$\underline{H}_3$). Spectroscopic data in accordance with the literature [86].

5.2.4 Synthesis of methyl 2,3-di-*O*-acetyl-4,6-*O*-benzylidene-α-D-glucopyranoside (**4**)

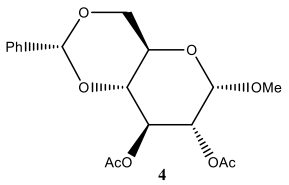

4

To a solution of **3** (6.49 g, 0.02 mol) in pyridine, acetic anhydride (32.58 mL, 0.34 mol) was added dropwise at 0 ºC, under nitrogen atmosphere. The reaction was followed by TLC using Cy/EtOAc (2:1), at room temperature. After 48 h, the reaction mixture was evaporated under reduced pressure and the resulting residue was extracted with DCM (3 x 200 mL) and water (200 mL). The organic layers were combined, dried with $MgSO_4$, the solids were filtered off and the filtrate concentrated in vacuum. Purification was achieved by recrystallization with ethyl ether, to give compound **4** (6.11 g) as white crystals in 80% yield. M.p. = 108 ºC – 109 ºC; $[\alpha]_D$ = + 6.7 (*c* 1.0, $CHCl_3$; Rf = 0.46 Cy/EtOAc (2:1); **^{1}H NMR** ($CDCl_3$, 400 MHz): δ 7.48 – 7.45 (m, 2H, H-aromatic), 7.39 – 7.36 (m, 3H, H-aromatic), 5.61 (t, 1H, H-3, $J_{3,4}$ = $J_{2,3}$ = 9.88Hz), 5.53 (s, 1H, H-7), 4.97 – 4.92 (m, 2H, H-1, H-2), 4.33 (dd, 1H, H-6a, $J_{6a,5}$ = 5.06Hz, $J_{6a,6b}$ = 10.18Hz), 3.95 (t, 1H, H-5, $J_{4,5}$ = $J_{6b,5}$ = 9.80Hz), 3.79 (t, 1H, H-6b), 3.67 (dd, 1H, H-4), 3.43 (s, 3H, -OC$\underline{H}_3$), 2.12 (s, 3H, -OCC$\underline{H}_3$), 2.07 (s, 3H, -OCC$\underline{H}_3$). Spectroscopic data in accordance with the literature [86].

5.2.5 Synthesis of methyl 2,3-di-*O*-acetyl-4-*O*-benzoyl-6-bromo-6-deoxy-α-D-glucopyranoside (**5**).

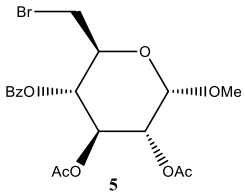

5

To a solution of **4** (0.14 g, 0.43 mmol) dissolved in CCl_4 (6 mL), *N*-bromosuccinimide (0.09 g, 0.51 mmol) and barium carbonate (0.23 g, 1.16 mmol), were added under nitrogen atmosphere. The mixture was heated under reflux and the reaction was followed by TLC, using Cy/EtOAc (2:1) as eluent. After 2.5 h, the reaction was cooled, filtered and extracted with DCM (2 x 100 mL) and water (100 mL). The organic layers were combined, dried with $MgSO_4$, the solids were filtered off and the filtrate concentrated in vacuum. Purification was achieved by chromatographic column, using Cy/EtOAc (8:1) as eluent, to afford compound **5** (0.10 g) as a colourless oil in 50% yield. Rf = 0.55 Cy/EtOAc (2:1), **^{1}H NMR** ($CDCl_3$, 400 MHz): δ 8.01 (dd, 1H, H-1´, $J_{1´,2´}$ = 7.13Hz, $J_{1´,3´}$ = 1.30Hz), 7.61 (t, 1H, H-2´, $J_{2´,3´}$ = 7.54Hz), 7.47 (t, 1H, H-3´), 5.71 (t, 1H, H-3, $J_{3,4}$ = 9.78Hz), 5.20 (t, 1H, H-4), 5.05 (d, 1H, H-1, $J_{1,2}$ =

3.59Hz), 4.98 (dd, 1H, H-2, $J_{2,3}$ = 10.41Hz), 4.17 – 4.12 (m, 1H, H-5), 3.54 – 3.43 (m, 5H, H-6ab, -OC$\underline{H}_3$), 2.10 (s, 3H, -OCC$\underline{H}_3$), 1.91 (s, 3H, -OCC$\underline{H}_3$). **^{13}C NMR** ($CDCl_3$, 400 MHz): δ 170.2 (-O$\underline{C}CH_3$), 169.9 (-O$\underline{C}CH_3$), 165.4 (C=O), 133.8 (C-2´), 129.9 (C-1´), 128.7 (C-3´), 96.7 (C-1), 71.6 (C-4), 70.9 (C-2), 69.5 (C-3), 69.0 (C-5), 55.6 (-O$\underline{C}H_3$), 31.4 (C-6), 20.8 (-OC$\underline{C}H_3$), 20.6 (-OC$\underline{C}H_3$).

6 References

1. Head, B. M., Rubinstein, E. & Meyers, A. F. A. Alternative pre-approved and novel therapies for the treatment of anthrax. *BMC Infect. Dis.* **16**, 621 (2016).
2. Bryskier, A. Bacillus anthracis and antibacterial agents. *Clin. Microbiol. Infect.* **8**, 467–478 (2002).
3. Lobanovska, M. & Pilla, G. Penicillin's Discovery and Antibiotic Resistance: Lessons for the Future? *Yale J. Biol. Med.* **90**, 135–145 (2017).
4. Dias, C. & Rauter, A. P. Membrane-targeting antibiotics: recent developments outside the peptide space. *Future Med. Chem.* **11**, 211–228 (2019).
5. Xavier, N. M. & Rauter, A. P. Environmentally friendly approaches to the synthesis of new antibiotics from sugars. *Pure Appl. Chem.* **84**, 803–816 (2012).
6. Rauter, A. P. *et al.* Synthesis, surface active and antimicrobial properties of new alkyl 2,6-dideoxy-l-arabino-hexopyranosides. *Carbohydr. Res.* **340**, 191–201 (2005).
7. Silva, F. V. M. *et al.* Alkyl deoxy-arabino-hexopyranosides: Synthesis, surface properties, and biological activities. *Bioorg. Med. Chem.* **16**, 4083–4092 (2008).
8. Martins, A. *et al.* Tuning the Bioactivity of Tensioactive Deoxy Glycosides to Structure: Antibacterial Activity Versus Selective Cholinesterase Inhibition Rationalized by Molecular Docking. *European J. Org. Chem.* **2013**, 1448–1459 (2013).
9. Dias, C. *et al.* Sugar-based bactericides targeting phosphatidylethanolamine-enriched membranes. *Nat. Commun.* **9**, 4857 (2018).
10. Dias, C. *et al.* Assessing the Optimal Deoxygenation Pattern of Dodecyl Glycosides for Antimicrobial Activity Against Bacillus anthracis. *European J. Org. Chem.* **2019**, 2224–2233 (2019).
11. Robyt, J. F. *Essentials of Carbohydrate Chemistry*. (Springer New York, 1998).
12. Carbohydrates, N. O. F. Nomenclature of Carbohydrates, (Recommendations 1996). in (1997).
13. Robert, S. & Williams, S. *Carbohydrates: The Essential Molecules of Life*. (Elsevier Science, 2008).
14. Davis, B. G. & Fairbanks, A. J. *Carbohydrate Chemistry*. (Oxford University Press, 2002).
15. Neuman, R. Carbohydrates. in *Organic Chemistry* (UCSB Chemistry, available online, 1992).
16. Bubb, W. A. NMR spectroscopy in the study of carbohydrates: Characterizing the structural complexity. *Concepts Magn. Reson. Part A Bridg. Educ. Res.* **19**, 1–19 (2003).
17. Wiberg, K. B., Bailey, W. F., Lambert, K. M. & Stempel, Z. D. The Anomeric Effect: It's Complicated. *J. Org. Chem.* **83**, 5242–5255 (2018).
18. Takahashi, O. *et al.* The Origin of the Relative Stability of Axial Conformers of Cyclohexane and Cyclohexanone Derivatives: Importance of the CH/n and CH/π Hydrogen Bonds. *Bull. Chem. Soc. Jpn.* **82**, 272–276 (2009).
19. Takahashi, O., Kohno, Y. & Nishio, M. Relevance of Weak Hydrogen Bonds in the Conformation of Organic Compounds and Bioconjugates: Evidence from Recent Experimental Data and High-Level ab Initio MO Calculations. *Chem. Rev.* **110**, 6049–6076 (2010).
20. Báti, G., He, J., Pal, K. B. & Liu, X. Stereo- and regioselective glycosylation with protection-less sugar derivatives: an alluring strategy to access glycans and natural products. *Chem. Soc. Rev.* **48**, 4006–4018 (2019).
21. Tanaka, M. *et al.* Boronic-Acid-Catalyzed Regioselective and 1,2- cis -Stereoselective Glycosylation of Unprotected Sugar Acceptors via SNi-Type Mechanism. *J. Am. Chem. Soc.* **140**, 3644–3651 (2018).
22. Elferink, H., Mensink, R. A., White, P. B. & Boltje, T. J. Stereoselective β-Mannosylation by Neighboring-Group Participation. *Angew. Chemie Int. Ed.* **55**, 11217–11220 (2016).
23. Frihed, T. G., Bols, M. & Pedersen, C. M. Mechanisms of Glycosylation Reactions Studied by Low-Temperature Nuclear Magnetic Resonance. *Chem. Rev.* **115**, 4963–5013 (2015).
24. Yao, H. *et al.* Catalyst-Controlled Stereoselective O -Glycosylation: Pd(0) vs Pd(II). *ACS Catal.* **7**, 5456–5460 (2017).
25. Chatterjee, S., Moon, S., Hentschel, F., Gilmore, K. & Seeberger, P. H. An Empirical Understanding of the Glycosylation Reaction. *J. Am. Chem. Soc.* **140**, 11942–11953 (2018).

26. Aslam, B. *et al.* Antibiotic resistance: a rundown of a global crisis. *Infect. Drug Resist.* **11**, 1645–1658 (2018).
27. Ritter, T. K. & Wong, C. Carbohydrate-Based Antibiotics: A New Approach to Tackling the Problem of Resistance. *Angew. Chemie Int. Ed.* **40**, 3508 (2001).
28. Auer, G. K. & Weibel, D. B. Bacterial Cell Mechanics. *Biochemistry* **56**, 3710–3724 (2017).
29. Lowy, F. D. Antimicrobial resistance: the example of Staphylococcus aureus. *J. Clin. Invest.* **111**, 1265–1273 (2003).
30. Silhavy, T. J., Kahne, D. & Walker, S. The Bacterial Cell Envelope. *Cold Spring Harb. Perspect. Biol.* **2**, a000414–a000414 (2010).
31. Goel, A. K. Anthrax: A disease of biowarfare and public health importance. *World J. Clin. Cases* **3**, 20 (2015).
32. Kock, R., Haider, N., Mboera, L. E. & Zumla, A. A One-Health lens for anthrax. *Lancet Planet. Heal.* **3**, e285–e286 (2019).
33. Halvorson, H. O. Two generations of spore research: from father to son. *Microbiologia* **13**, 131–48 (1997).
34. Jernigan, J. Bioterrorism-Related Inhalational Anthrax: The First 10 Cases Reported in the United States. *Emerg. Infect. Dis.* **7**, 933–944 (2001).
35. Schitter, G. & Wrodnigg, T. M. Update on carbohydrate-containing antibacterial agents. *Expert Opin. Drug Discov.* **4**, 315–356 (2009).
36. Serio, A. W., Magalhães, M. L., Blanchard, J. S. & Connolly, L. E. *Antimicrobial Drug Resistance*. (Springer International Publishing, 2017).
37. Udou, T. Dissemination of nosocomial multiple-aminoglycoside-resistant Staphylococcus aureus caused by horizontal transfer of the resistance determinant (aacA/aphD) and clonal spread of resistant strains. *Am. J. Infect. Control* **32**, 215–219 (2004).
38. Thwaites, M. *et al.* Evaluation of the Bactericidal Activity of Plazomicin and Comparators against Multidrug-Resistant Enterobacteriaceae. *Antimicrob. Agents Chemother.* **62**, (2018).
39. Saravolatz, L. D. & Stein, G. E. Plazomicin: A New Aminoglycoside. *Clin. Infect. Dis.* (2019).
40. Kimura, K. & Bugg, T. D. H. Recent advances in antimicrobial nucleoside antibiotics targeting cell wall biosynthesis. *Nat. Prod. Rep.* **20**, 252–273 (2003).
41. Thomson, J. M. & Lamont, I. L. Nucleoside Analogues as Antibacterial Agents. *Front. Microbiol.* **10**, (2019).
42. Niu, G., Li, Z., Huang, P. & Tan, H. Engineering nucleoside antibiotics toward the development of novel antimicrobial agents. *J. Antibiot. (Tokyo).* **72**, 906–912 (2019).
43. Blaskovich, M. A. T. *et al.* Developments in Glycopeptide Antibiotics. *ACS Infect. Dis.* **4**, 715–735 (2018).
44. Dinos, G. P. The macrolide antibiotic renaissance. *Br. J. Pharmacol.* **174**, 2967–2983 (2017).
45. Kiely, D. E. Carbohydrate Chemistry: Proven Synthetic Methods, Vol 3, Proven Synthetic Methods Series, Pavol Kováč, Ed. *Glycoconj. J.* **32**, 655–656 (2015).
46. Ferrier, R. J. & Zubkov, O. A. Transformation of Glycals into 2,3-Unsaturated Glycosyl Derivatives. in *Organic Reactions* 569–736 (John Wiley & Sons, Inc., 2003).
47. Guo, J. & Ye, X.-S. Protecting Groups in Carbohydrate Chemistry: Influence on Stereoselectivity of Glycosylations. *Molecules* **15**, 7235–7265 (2010).
48. de Lederkremer, R. M. & Marino, C. Deoxy Sugars: Occurrence and Synthesis. in *Advances in Carbohydrate Chemistry and Biochemistry* 143–216 (Elsevier Inc., 2007).
49. Pozsgay, V. & Neszmélyi, A. Synthesis and carbon-13NMR-spectral study of methyl 2,6- and 3,6-dideoxy-α-L-arabino- and methyl 4,6-dideoxy-α-L-lyxo-hexopyranoside. *Carbohydr. Res.* **85**, 143–150 (1980).
50. Barton, D. H. R. & McCombie, S. W. A new method for the deoxygenation of secondary alcohols. *J. Chem. Soc. Perkin Trans. 1* 1574 (1975).
51. Siewert, G. & Westphal, O. Substitution sekundärer Tosylestergruppen durch Jod Synthese von 4-Desoxy- und 4.6-Didesoxy-D-xylo-hexose. *Justus Liebigs Ann. Chem.* **720**, 161–170 (1968).
52. Wessel, H. P., Viaud, M.-C. & Gardon, V. Preparation of 4,6-cyclo-4,6-dideoxy-hexopyranoses by palladium-mediated intramolecular cyclodehalogenation. *Carbohydr. Res.* **245**, 233–244 (1993).
53. Wessel, H. P., Minder, R. & Trumtel, M. The synthesis of four dideoxygenated analogues of β-

maltosyl-(1→4)-trehalose. *J. Carbohydr. Chem.* **17**, 1283–1306 (1998).
54. Crotti, P., Di Bussolo, V., Favero, L., Macchia, F. & Pineschi, M. Regiochemical control of the ring opening of 1,2-epoxides by means of chelating processes. Part 17: Synthesis and opening reactions of cis- and trans-oxides derived from (2S,6R)-2-benzyloxy-6-methyl-3,6-dihydro-2H-pyran, (2R,6R)- and (2S,6R)-2-methoxy-6-m. *Tetrahedron* **58**, 6069–6091 (2002).
55. Lawton, B. T., Szarek, W. A. & Jones, J. K. N. A facile synthesis of 4,6-dideoxy-D-xylo-hexose. *Carbohydr. Res.* **14**, 255–258 (1970).
56. Danishefsky, S. & Kerwin, J. F. A simple synthesis of dl-chalcose. *J. Org. Chem.* **47**, 1597–1598 (1982).
57. Sharpless, K. B. *et al.* The osmium-catalyzed asymmetric dihydroxylation: a new ligand class and a process improvement. *J. Org. Chem.* **57**, 2768–2771 (1992).
58. Sun, J. *et al.* The total synthesis of D-chalcose and its C-3 epimer. *Beilstein J. Org. Chem.* **9**, 2620–2624 (2013).
59. Fraser-Reid, B. O., Tatsuta, K. & Thiem, J. *Glycoscience Chemistry and Chemical Biology*. (Springer, 2008).
60. Yang, Y. & Yu, B. Recent Advances in the Chemical Synthesis of C -Glycosides. *Chem. Rev.* **117**, 12281–12356 (2017).
61. Matos, A. M. *et al.* Synthesis and effects of flavonoid structure variation on amyloid-β aggregation. *Pure Appl. Chem.* **89**, 1305–1320 (2017).
62. Rauter, A. P. *et al.* Liquid chromatography–diode array detection–electrospray ionisation mass spectrometry/nuclear magnetic resonance analyses of the anti-hyperglycemic flavonoid extract of Genista tenera. *J. Chromatogr. A* **1089**, 59–64 (2005).
63. Rauter, A. P., Lopes, R. G. & Martins, A. C -Glycosylflavonoids: Identification, Bioactivity and Synthesis. *Nat. Prod. Commun.* **2**, (2007).
64. Xie, Y., Yang, W., Tang, F., Chen, X. & Ren, L. Antibacterial Activities of Flavonoids: Structure-Activity Relationship and Mechanism. *Curr. Med. Chem.* **22**, 132–149 (2014).
65. Tagousop, C. N., Tamokou, J.-D., Ekom, S. E., Ngnokam, D. & Voutquenne-Nazabadioko, L. Antimicrobial activities of flavonoid glycosides from Graptophyllum grandulosum and their mechanism of antibacterial action. *BMC Complement. Altern. Med.* **18**, 252 (2018).
66. Liao, H., Ma, J., Yao, H. & Liu, X. W. Recent progress of: C -glycosylation methods in the total synthesis of natural products and pharmaceuticals. *Org. Biomol. Chem.* **16**, 1791–1806 (2018).
67. Roy, R., Tropper, F. D., Cao, S. & Kim, J. M. Anomeric Group Transformations Under Phase-Transfer Catalysis. in 163–180 (1997).
68. G. dos Santos, R., R. Jesus, A., M. Caio, J. & P. Rauter, A. Fries-type Reactions for the C-Glycosylation of Phenols. *Curr. Org. Chem.* **15**, 128–148 (2011).
69. Zeng, J., Ma, J., Xiang, S., Cai, S. & Liu, X.-W. Stereoselective β-C-Glycosylation by a Palladium-Catalyzed Decarboxylative Allylation: Formal Synthesis of Aspergillide A. *Angew. Chemie Int. Ed.* **52**, 5134–5137 (2013).
70. Bouvet, V. R. & Ben, R. N. A Short and Economical Synthesis of Orthogonally Protected C -Linked 2-Deoxy-2-acetamido-α-D-galactopyranose Derivatives. *J. Org. Chem.* **71**, 3619–3622 (2006).
71. Hager, D., Mayer, P., Paulitz, C., Tiebes, J. & Trauner, D. Stereoselective Total Syntheses of Herbicidin C and Aureonuclemycin through Late-Stage Glycosylation. *Angew. Chemie Int. Ed.* **51**, 6525–6528 (2012).
72. Kitamura, K. *et al.* Synthesis of the Pluramycins 2: Total Synthesis and Structure Assignment of Saptomycin B. *Angew. Chemie Int. Ed.* **53**, 1262–1265 (2014).
73. Du Toit, J. I., Van Sittert, C. G. C. E. & Vosloo, H. C. M. Metal carbenes in homogeneous alkene metathesis: Computational investigations. *J. Organomet. Chem.* **738**, 76–91 (2013).
74. Occhipinti, G. & Jensen, V. R. Nature of the Transition Metal–Carbene Bond in Grubbs Olefin Metathesis Catalysts. *Organometallics* **30**, 3522–3529 (2011).
75. Grubbs, R. H., Trnka, T. M. & Sanford, M. S. Transition Metal–Carbene Complexes in Olefin Metathesis and Related Reactions. in 187–231 (2003).
76. Adlhart, C. & Chen, P. Ligand Rotation Distinguishes First- and Second-Generation Ruthenium Metathesis Catalysts. *Angew. Chemie Int. Ed.* **41**, 4484–4487 (2002).
77. Nelson, D. J., Manzini, S., Urbina-Blanco, C. A. & Nolan, S. P. Key processes in ruthenium-

catalysed olefin metathesis. *Chem. Commun.* **50**, 10355–10375 (2014).
78. Ashworth, I. W., Hillier, I. H., Nelson, D. J., Percy, J. M. & Vincent, M. A. What is the initiation step of the Grubbs-Hoveyda olefin metathesis catalyst? *Chem. Commun.* **47**, 5428 (2011).
79. Love, J. A., Morgan, J. P., Trnka, T. M. & Grubbs, R. H. A Practical and Highly Active Ruthenium-Based Catalyst that Effects the Cross Metathesis of Acrylonitrile. *Angew. Chemie Int. Ed.* **41**, 4035–4037 (2002).
80. Johnsson, R. A., Bogojeski, J. J. & Damha, M. J. An evaluation of selective deprotection conditions for the synthesis of RNA on a light labile solid support. *Bioorg. Med. Chem. Lett.* **24**, 2146–2149 (2014).
81. Hanessian, S. The reaction products are versatile intermediates for further synthetic work in the carbohydrate series since they possess the combined advantages of a good leaving- group at. *Carbohydr. Res.* **2**, 86–88 (1966).
82. McNulty, J., Wilson, J. & Rochon, A. C. Regiocontrol in the Oxidative Radical Fragmentation of Benzilidene Acetals and Its Mechanistic Implications. *J. Org. Chem.* **69**, 563–565 (2004).
83. Crich, D. & Bowers, A. A. 4,6-O-[1-Cyano-2-(2-iodophenyl)ethylidene] Acetals. Improved Second-Generation Acetals for the Stereoselective Formation of β-D-Mannopyranosides and Regioselective Reductive Radical Fragmentation to β-D-Rhamnopyranosides. Scope and Limitations. *J. Org. Chem.* **71**, 3452–3463 (2006).
84. Liotta, L. J., Dombi, K. L., Kelley, S. A., Targontsidis, S. & Morin, A. M. Substituted benzyl ethers as radical stable protecting groups. *Tetrahedron Lett.* **38**, 7833–7834 (1997).
85. Barili, P. L. *et al.* 4,6-O-Benzylidene-d-glucopyranose and its sodium salt: new data on their preparation and properties. *Carbohydr. Res.* **278**, 43–57 (1995).
86. Demchenko, A. V., Pornsuriyasak, P. & De Meo, C. Acetal protecting groups in the organic laboratory: Synthesis of methyl 4,6-O-benzylidene-α-D-glucopyranoside. *J. Chem. Educ.* **83**, 782–784 (2006).
87. Bartlett, P. A. & Johnson, W. S. An improved reagent for the O-alkyl cleavage of methyl esters by nucleophilic displacement. *Tetrahedron Lett.* **11**, 4459–4462 (1970).

7 Annexes

7.1 Overall synthetic schemes

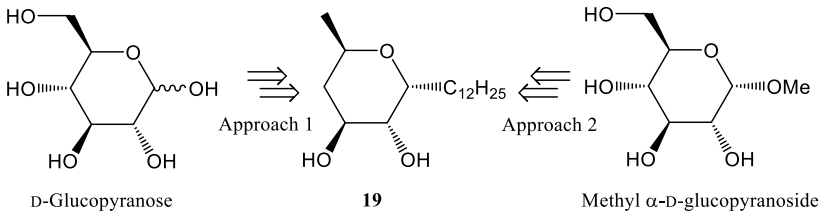

*Scheme 7.1. Starting materials used in approaches 1 and 2 to synthesize C-glycoside **19**.*

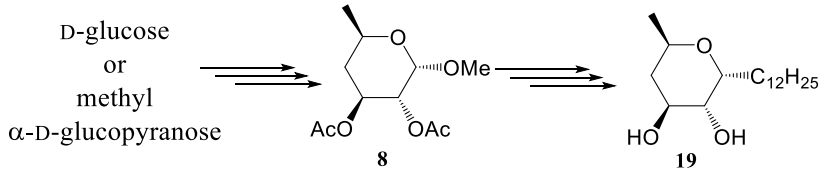

Scheme 7.2. General scheme of the steps pursued from two different starting materials in the development of the synthetic route towards the dodecyl 4,6-dideoxy glycoside.

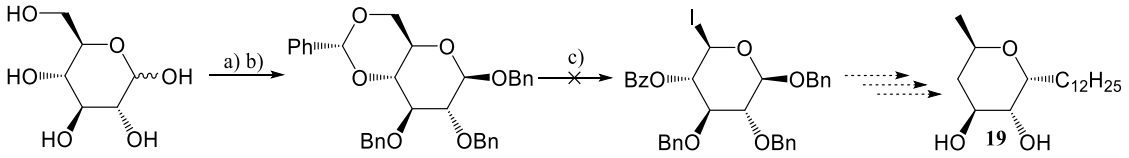

Scheme 7.3. Detailed approach 1. Reagents and conditions: a) $PhCH(OCH_3)_2$, p-TSA, DMF; b) BnBr, NaH, DMF, 6% yield (over two steps); c) NIS, CCl_4, $BaCO_3$.

7.2 NMR spectra

7.2.1 NMR spectra of 4,6-*O*-benzylidene-D-glucopyranose (**1a/b**).

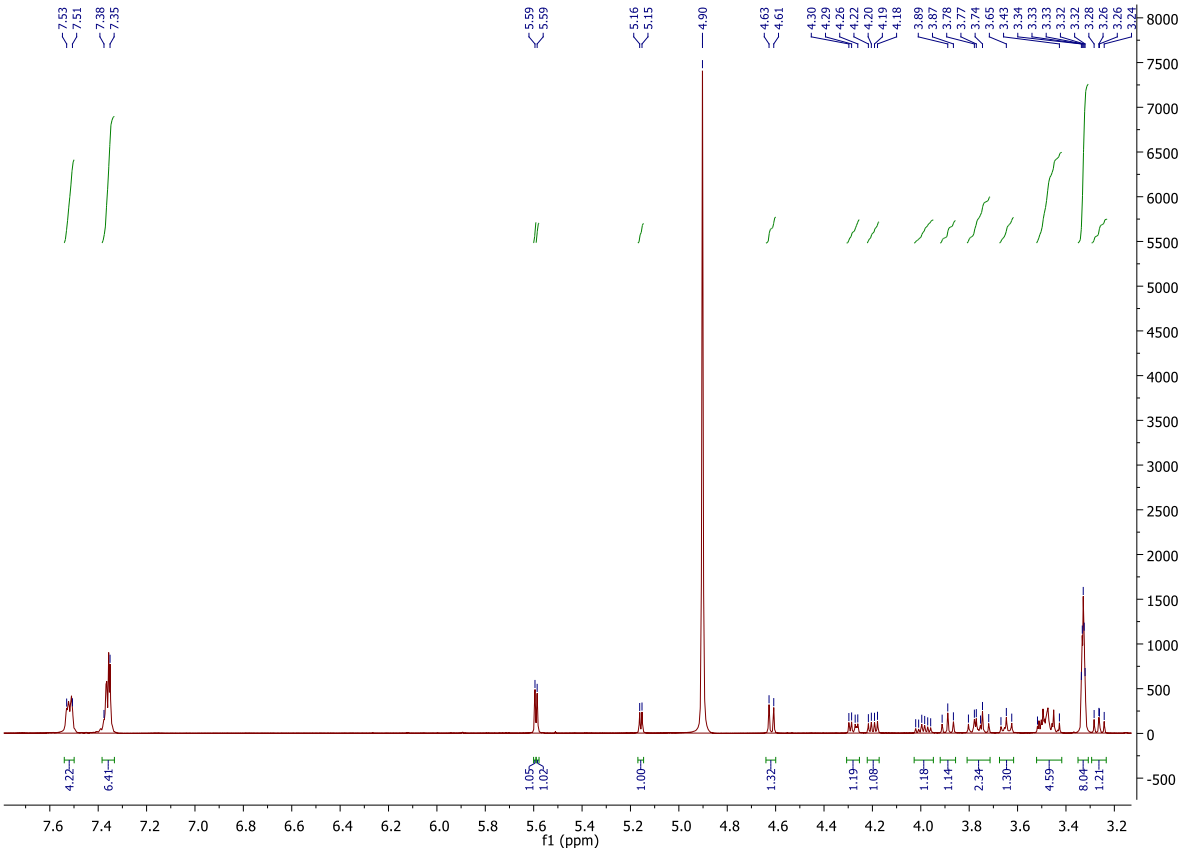

*Figure 7.1. [1]H NMR spectrum of compounds **1a/b**, in MeOD.*

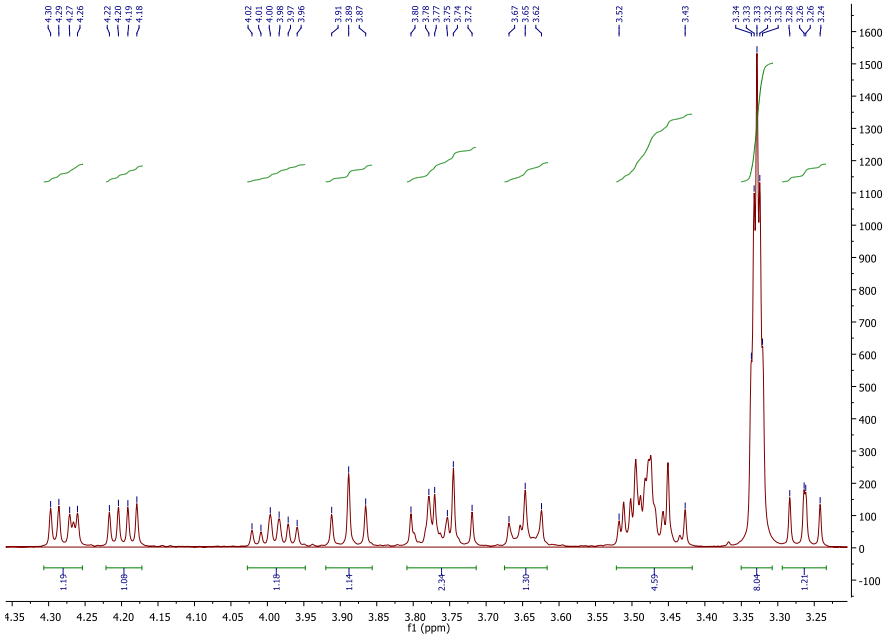

*Figure 7.2. Expansion of the [1]H NMR spectrum of compound **1a/b**, in MeOD, of the region between δ 3.25 ppm and δ 4.35 ppm.*

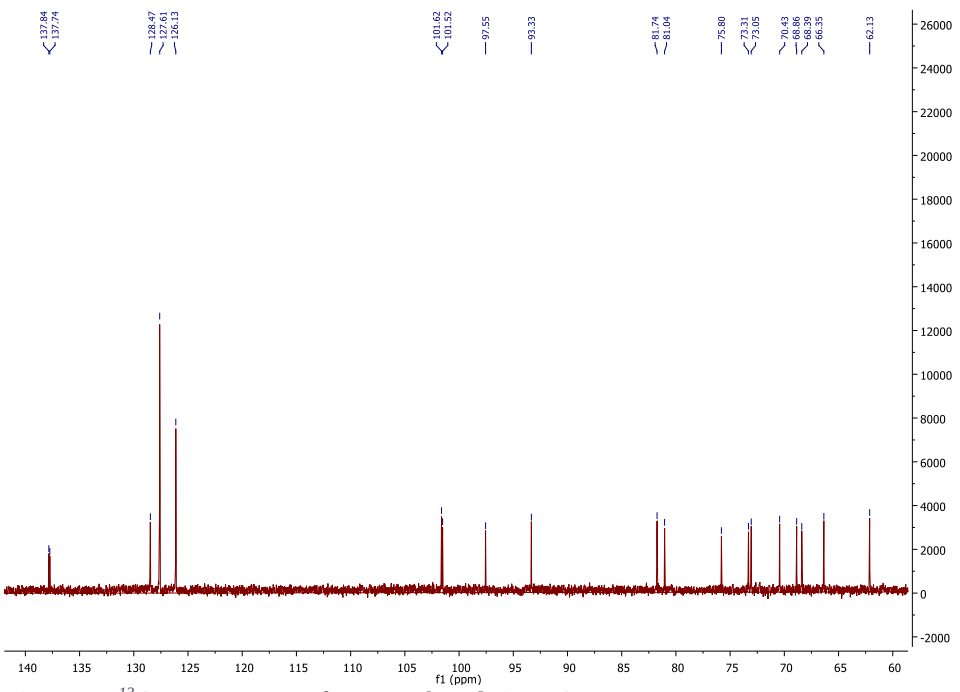

*Figure 7.3. ^{13}C NMR spectrum of compounds **1a/b**, in MeOD.*

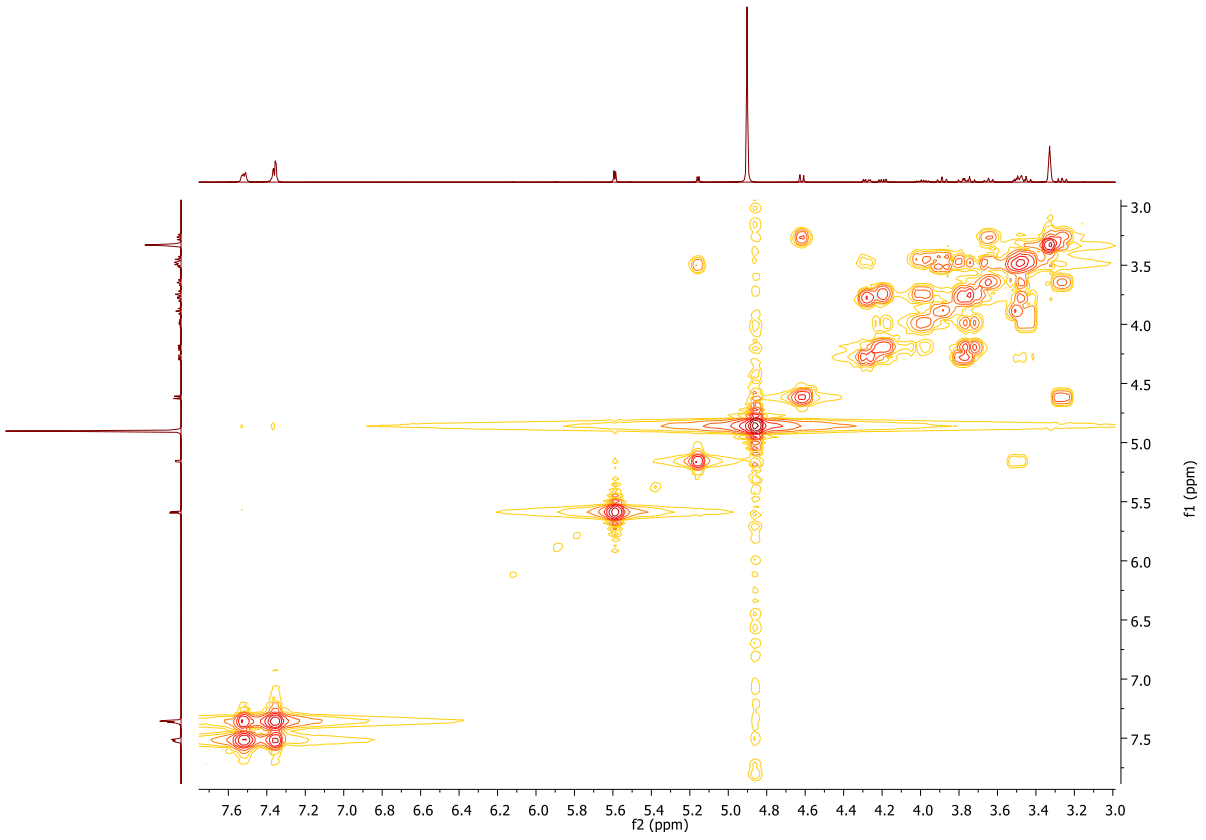

*Figure 7.4. COSY spectrum of compounds **1a/b**, in MeOD.*

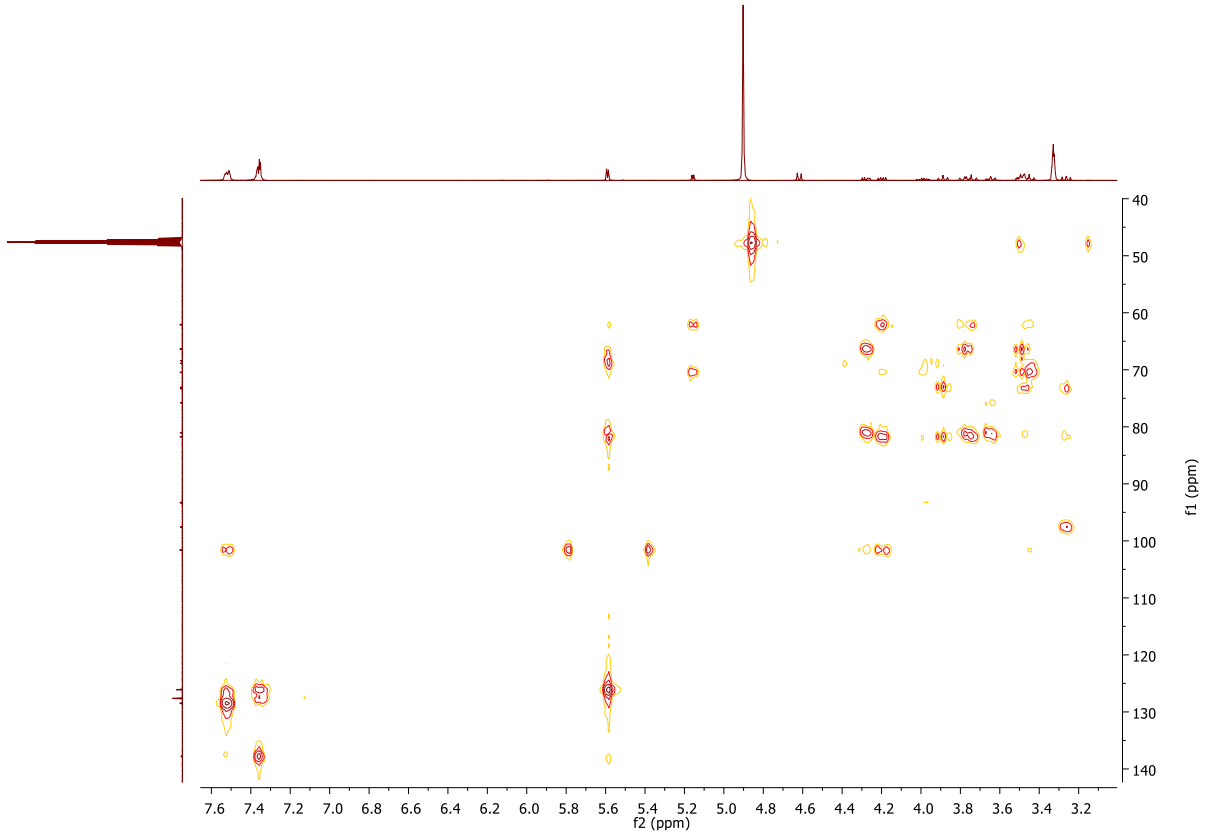

*Figure 7.5. HMBC spectrum of compounds **1a/b**, in MeOD.*

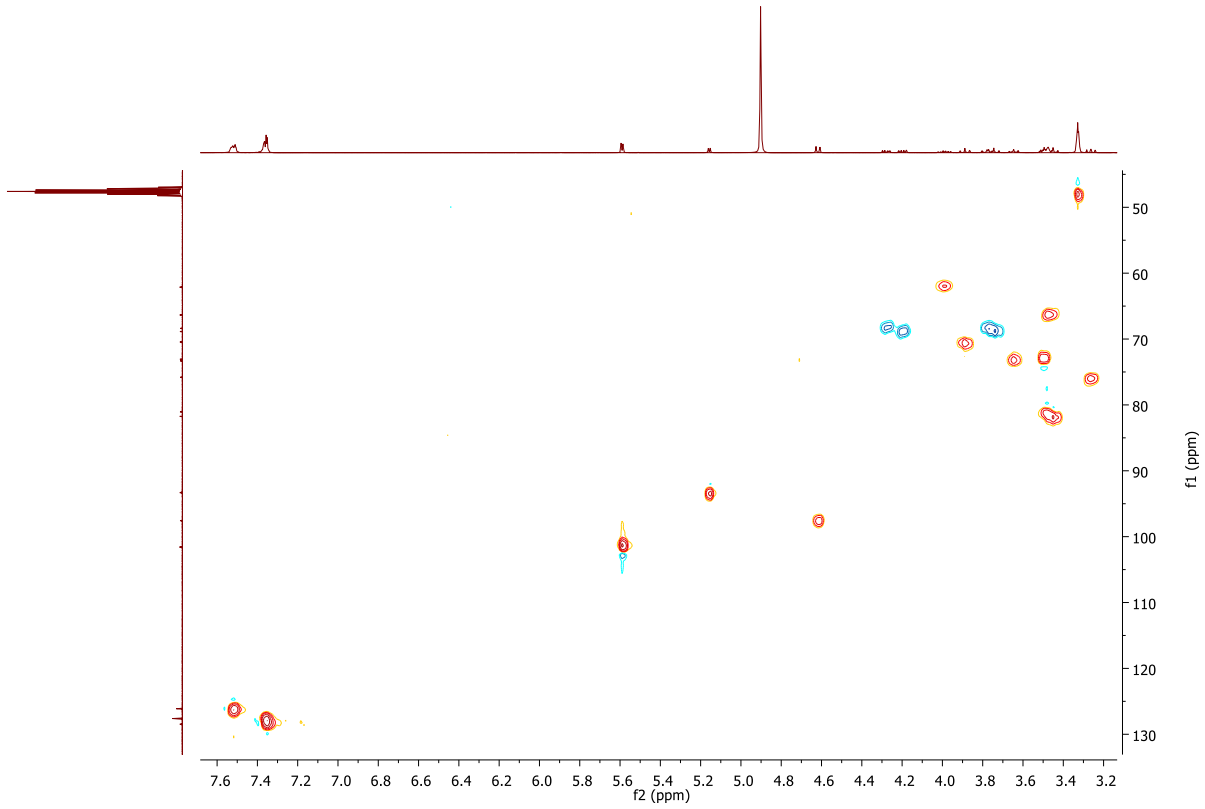

*Figure 7.6. HSQC spectrum of compounds **1a/b**, in MeOD.*

7.2.2 NMR spectra of benzyl 2,3-di-*O*-benzyl-4,6-*O*-benzylidene-α-D-glucopyranoside (**2**).

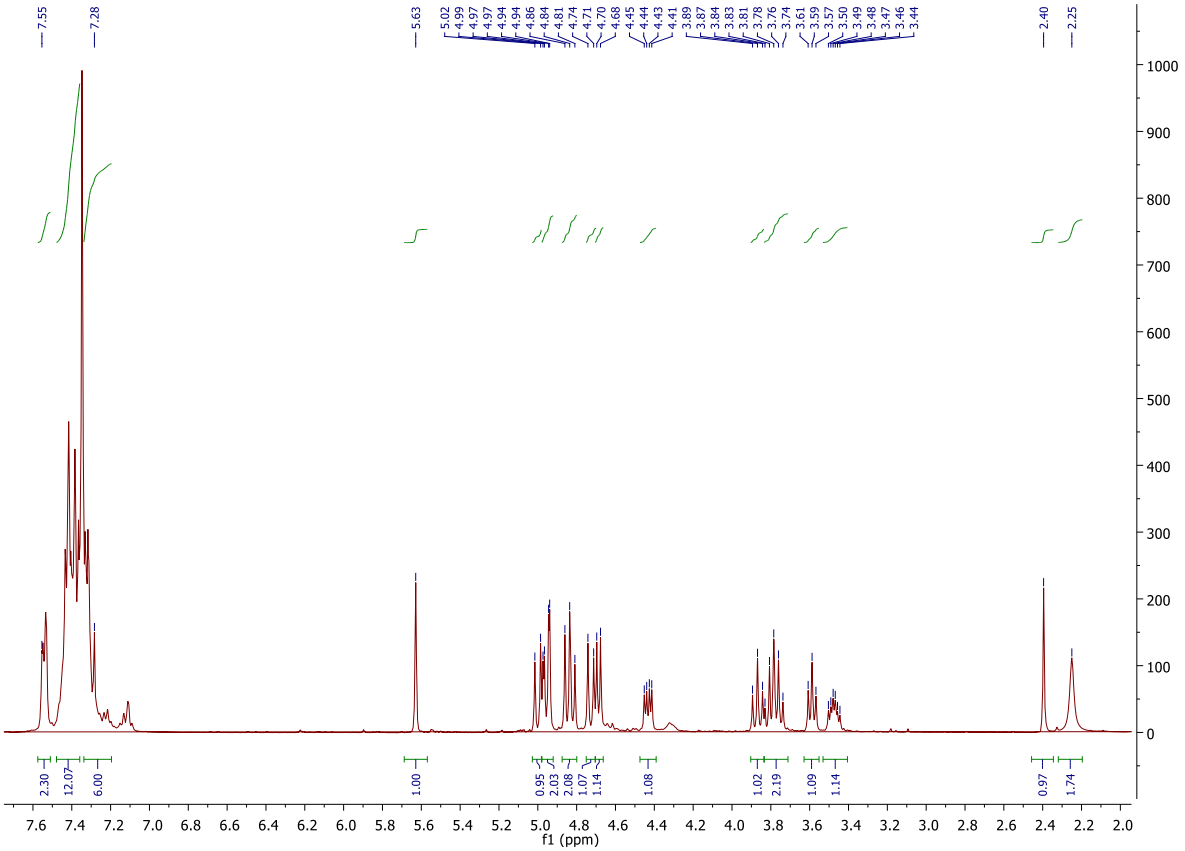

*Figure 7.7. ^{1}H NMR spectrum of compound **2**, in $CDCl_3$.*

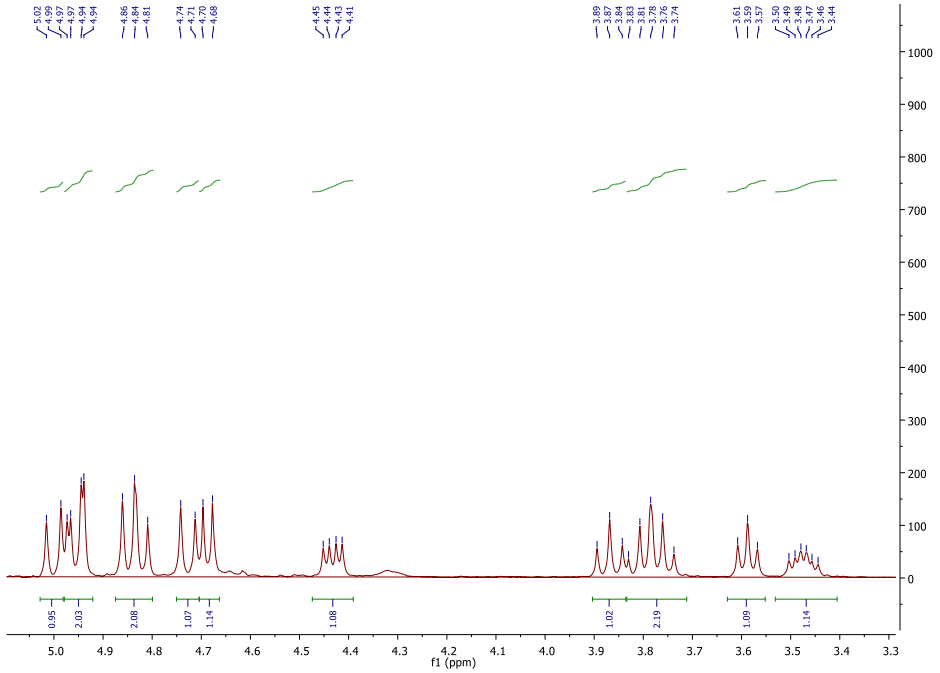

*Figure 7.8. Expansion of the ^{1}H NMR spectrum of compound **2**, in $CDCl_3$, of the region between δ 3.30 ppm and δ 5.05 ppm.*

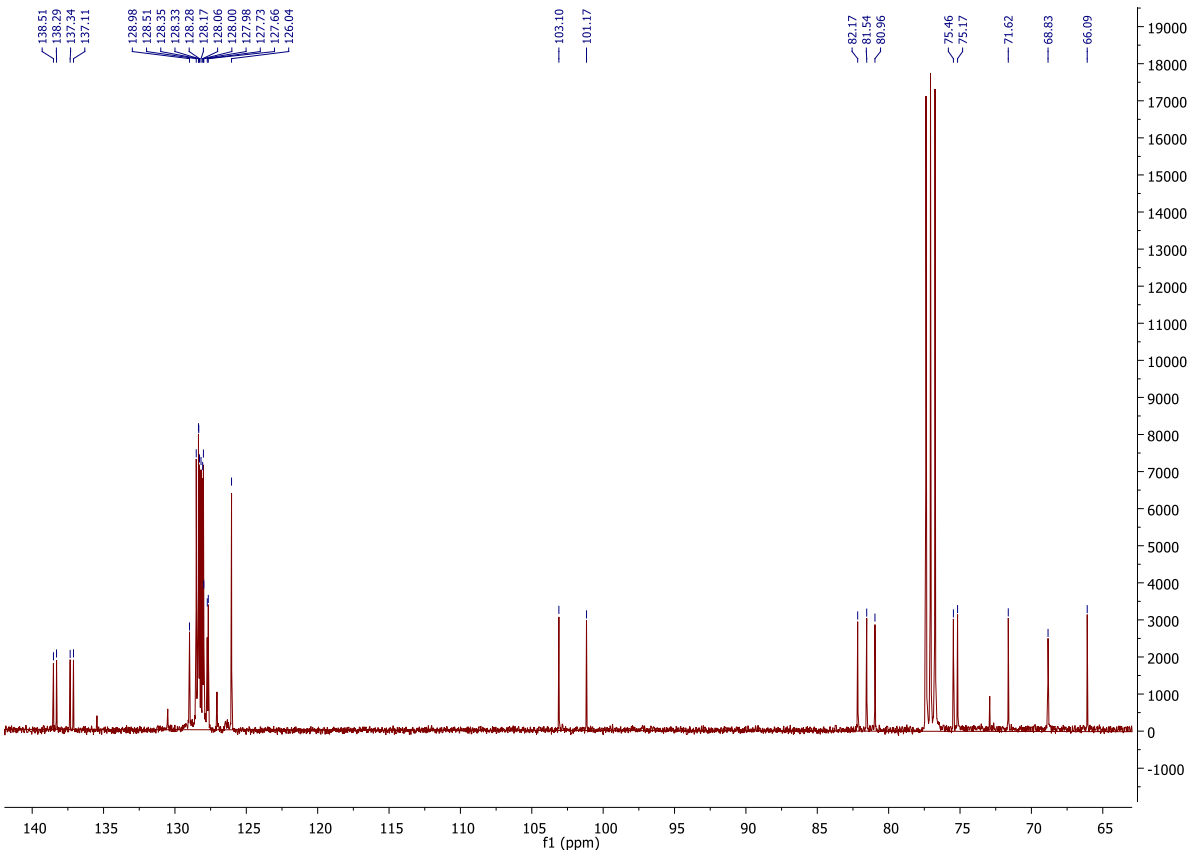

*Figure 7.9. ^{13}C NMR spectrum of compound **2**, in $CDCl_3$.*

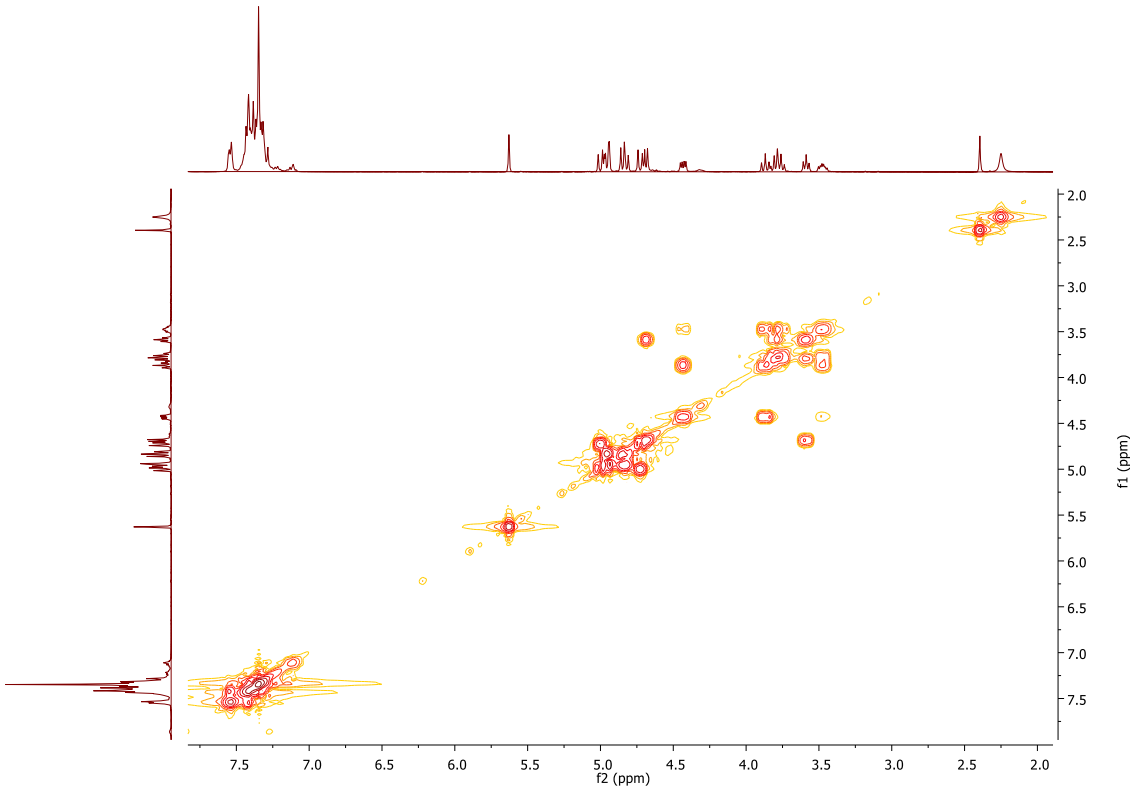

*Figure 7.10. COSY spectrum of compound **2**, in $CDCl_3$.*

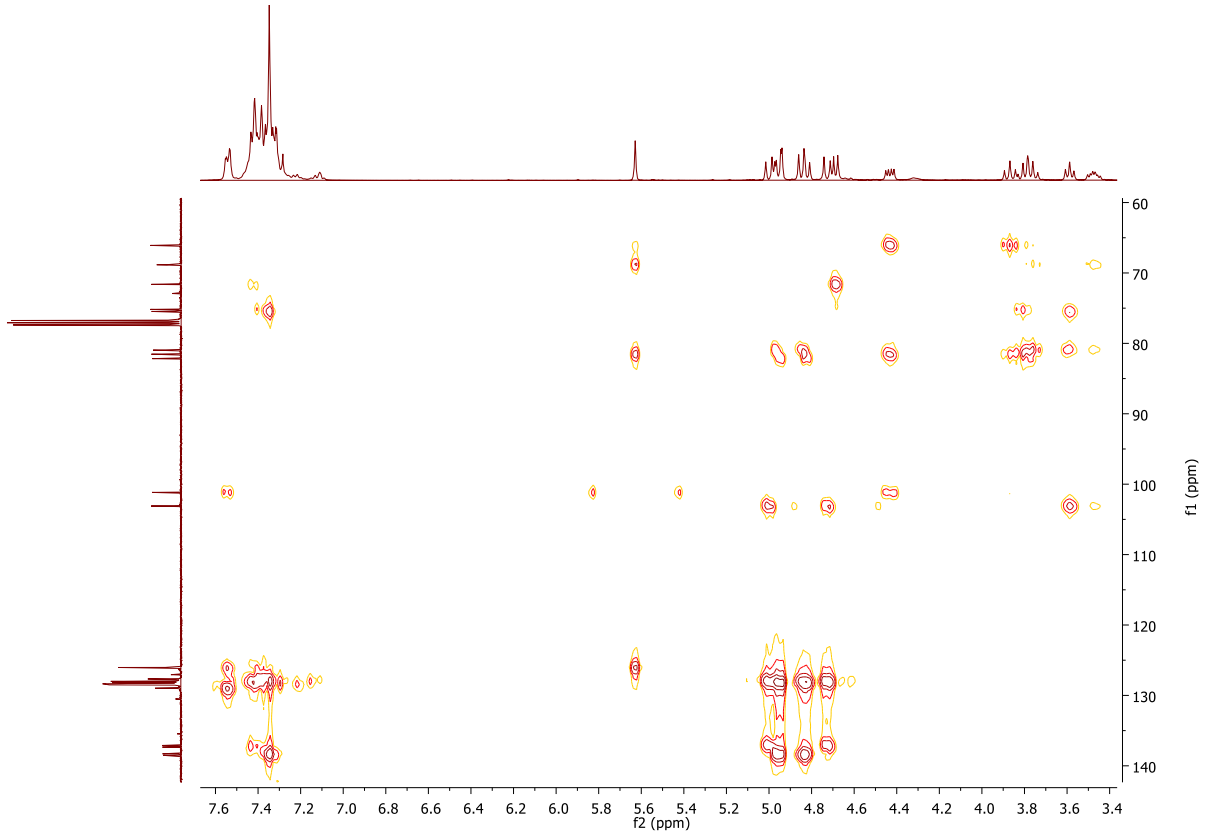

*Figure 7.11. HMBC spectrum of compound **2**, in $CDCl_3$.*

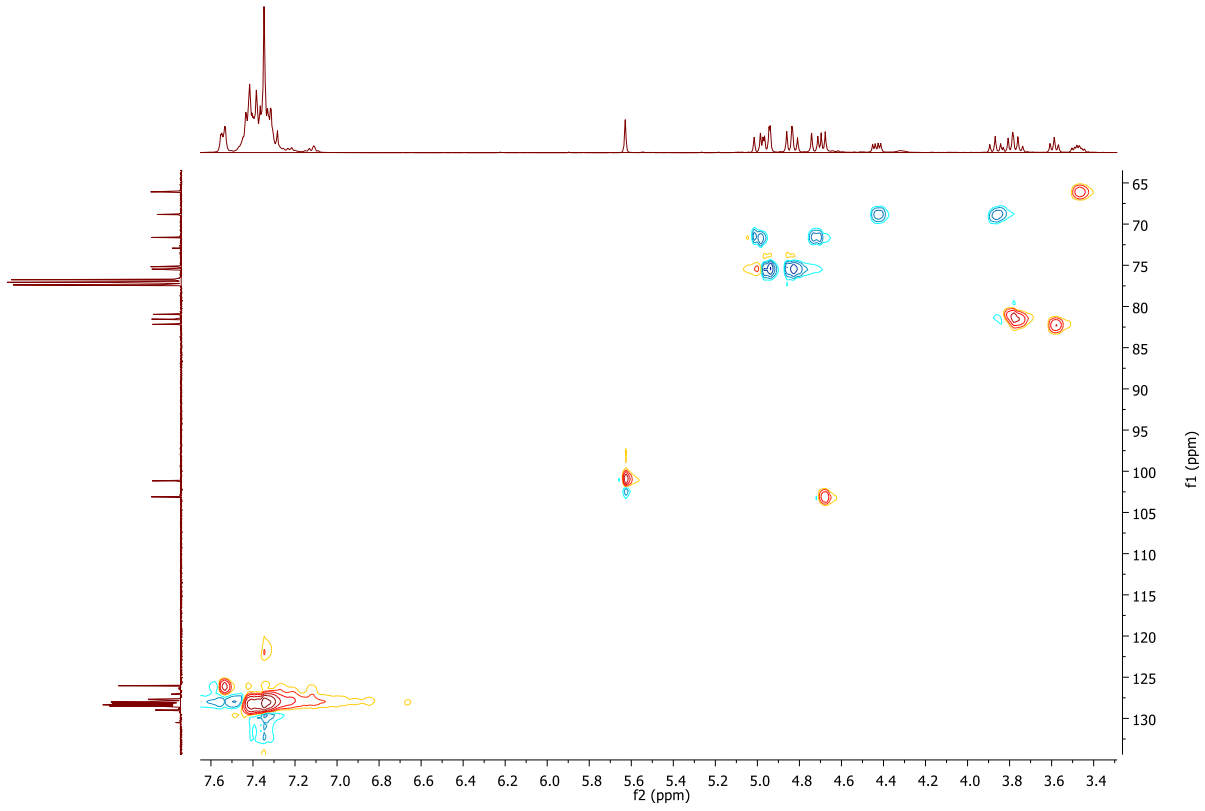

*Figure 7.12. HSQC spectrum of compound **2**, in $CDCl_3$.*

7.2.3 NMR spectrum of methyl 4,6-*O*-benzylidene-α-D-glucopyranoside (**3**).

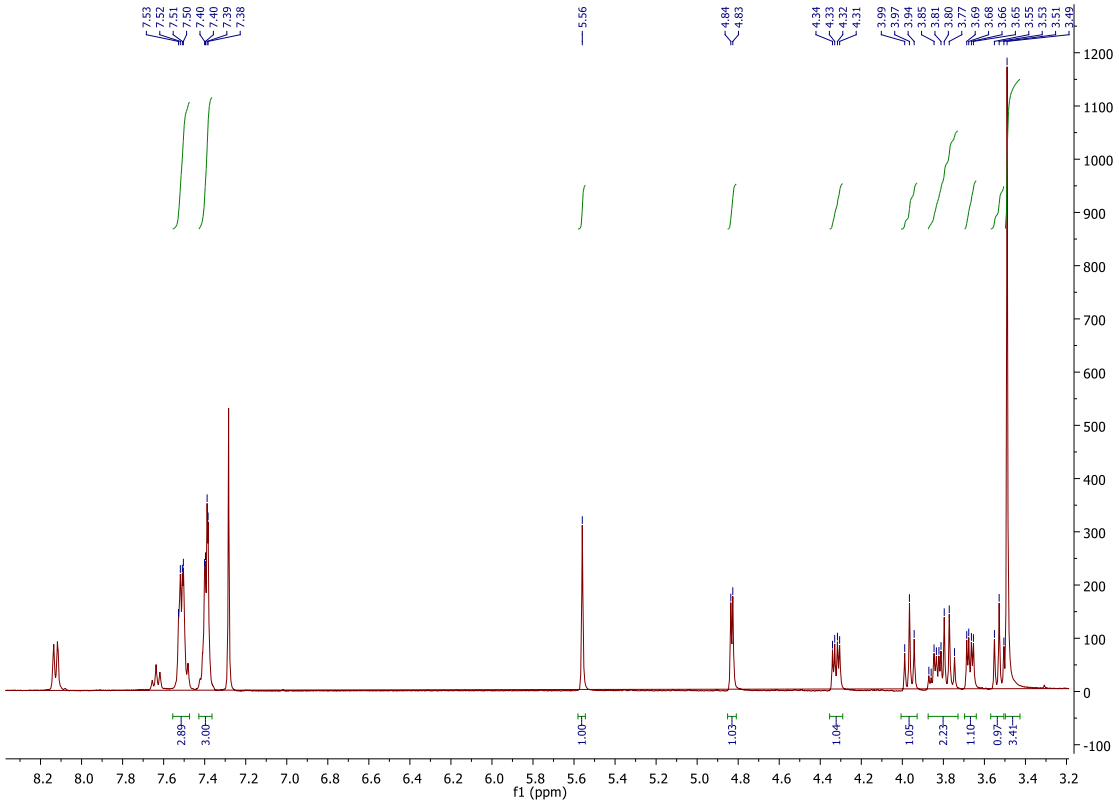

*Figure 7.13. ^{1}H NMR spectrum of compound **3**, in $CDCl_3$.*

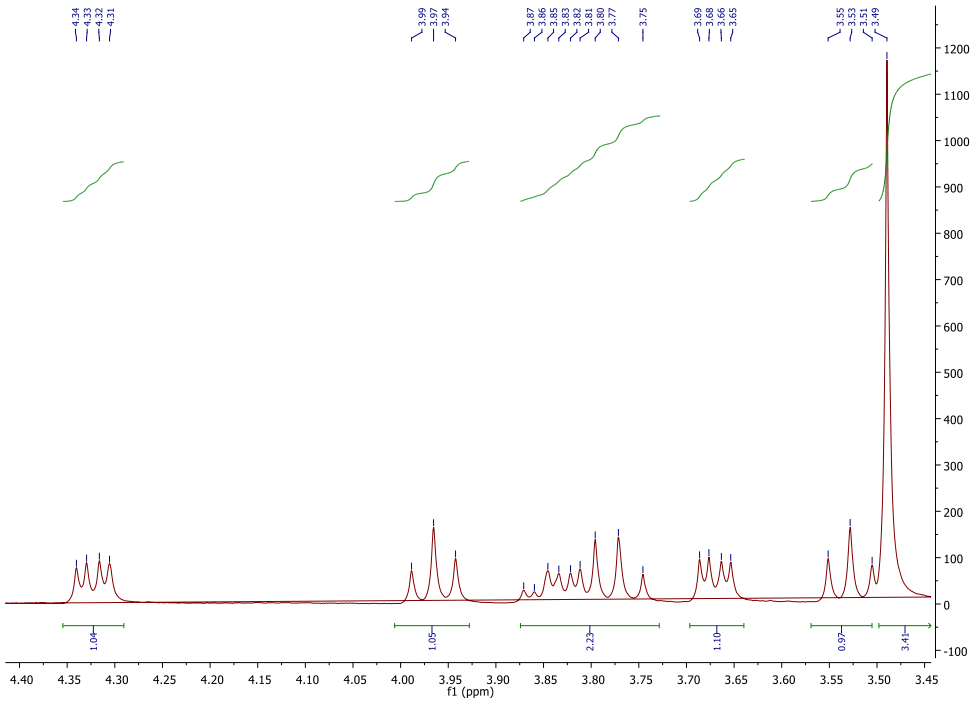

*Figure 7.14. Expansion of the ^{1}H NMR spectrum of compound **3**, in $CDCl_3$, of the region between δ 3.45 ppm and δ 4.40 ppm.*

7.2.4 NMR spectrum of methyl 2,3-di-*O*-acetyl-4,6-*O*-benzylidene-α-D-glucopyranoside (**4**).

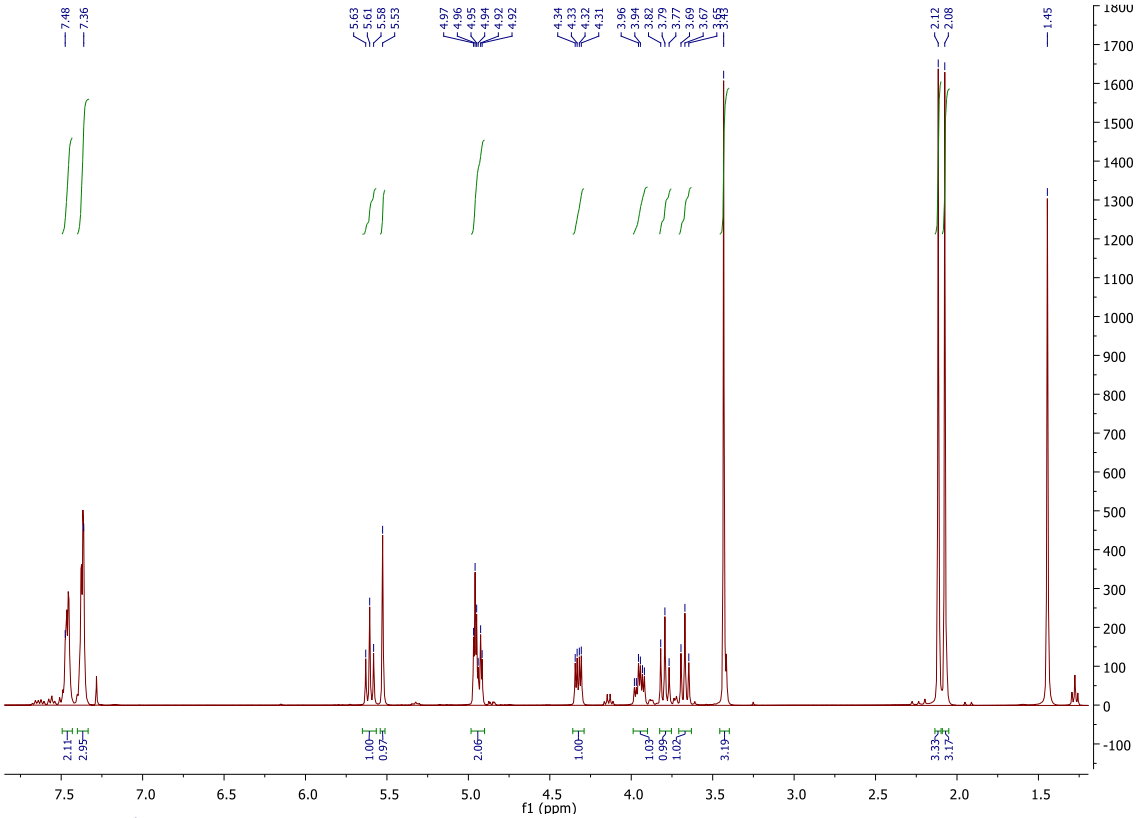

*Figure 7.15. ^{1}H NMR spectrum of compound **4**, in $CDCl_3$.*

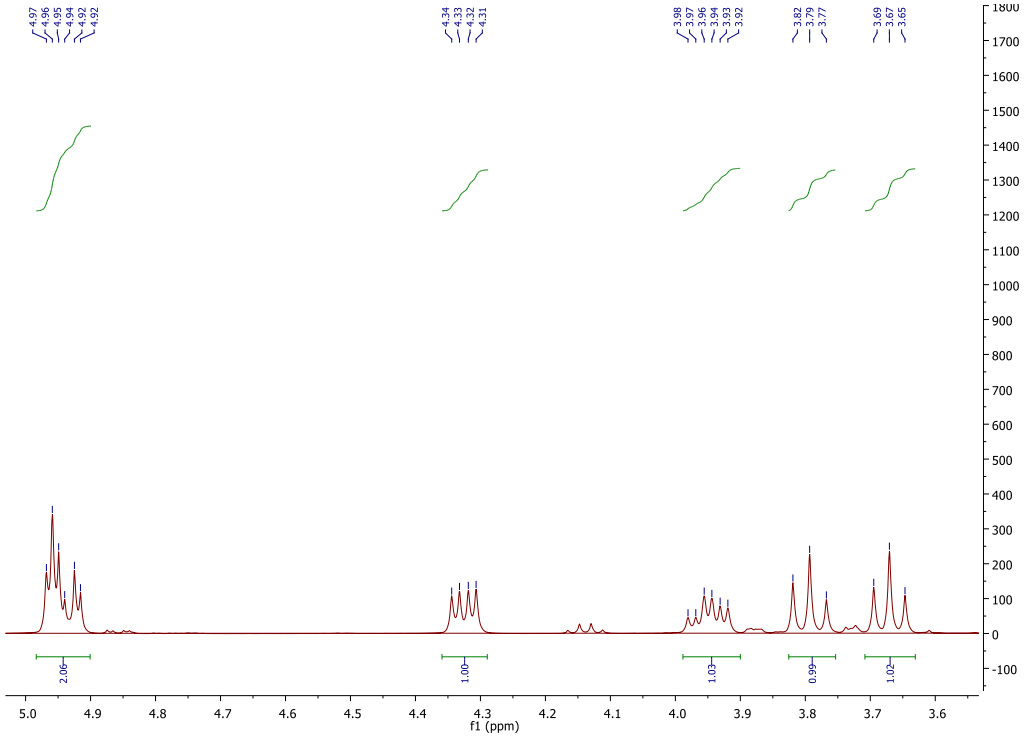

*Figure 7.16. Expansion of the ^{1}H NMR spectrum of compound **4**, in $CDCl_3$, of the region between δ 3.60 ppm and δ 5.00 ppm.*

7.2.5 NMR spectra of methyl 2,3-di-*O*-acetyl-4-*O*-benzoyl-6-bromo-6-deoxy-α-D-glucopyranoside (**5**).

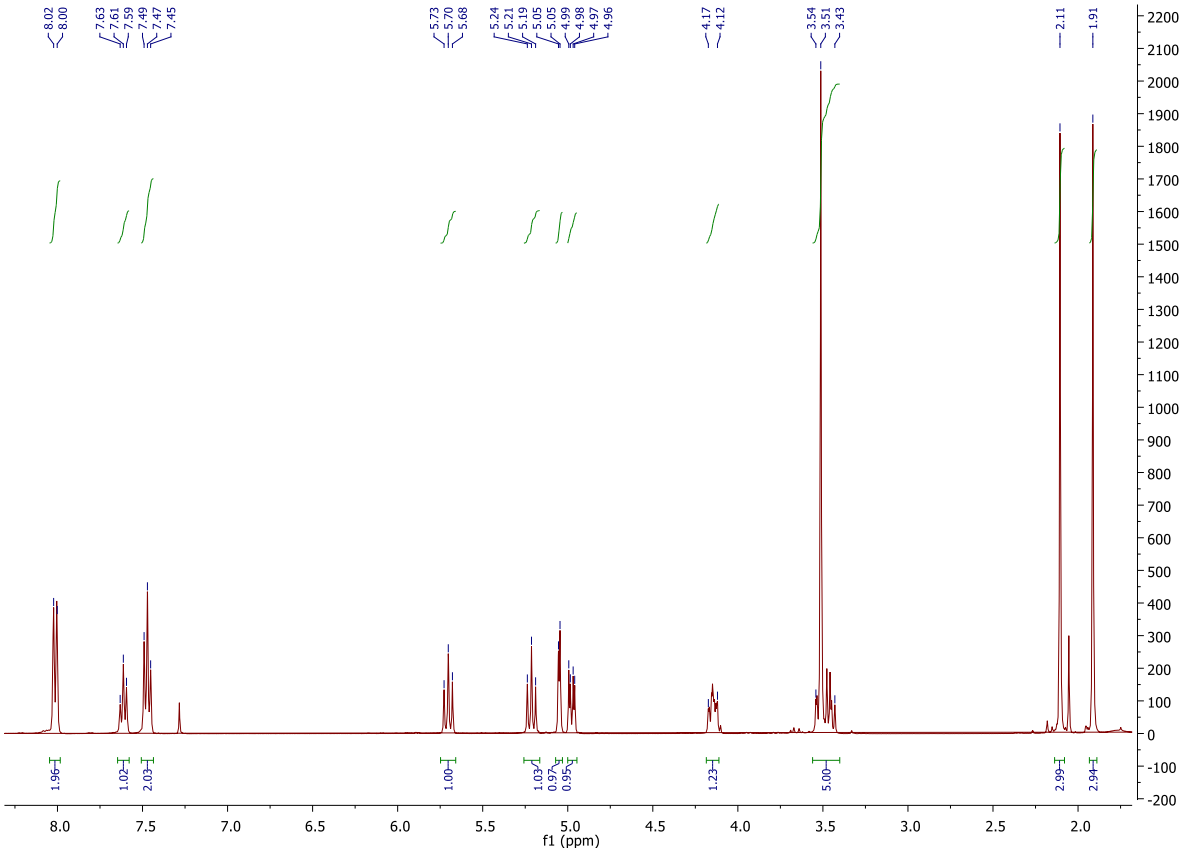

*Figure 7.17. [1]H NMR spectrum of compound **5**, in $CDCl_3$.*

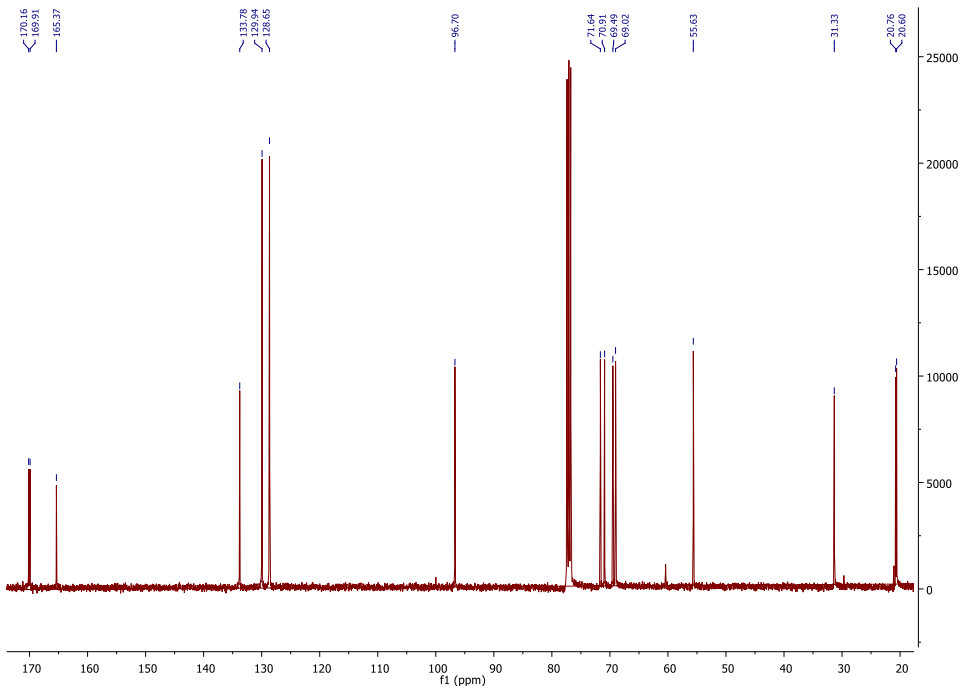

*Figure 7.18. [13]C NMR spectrum of compound **5**, in $CDCl_3$.*

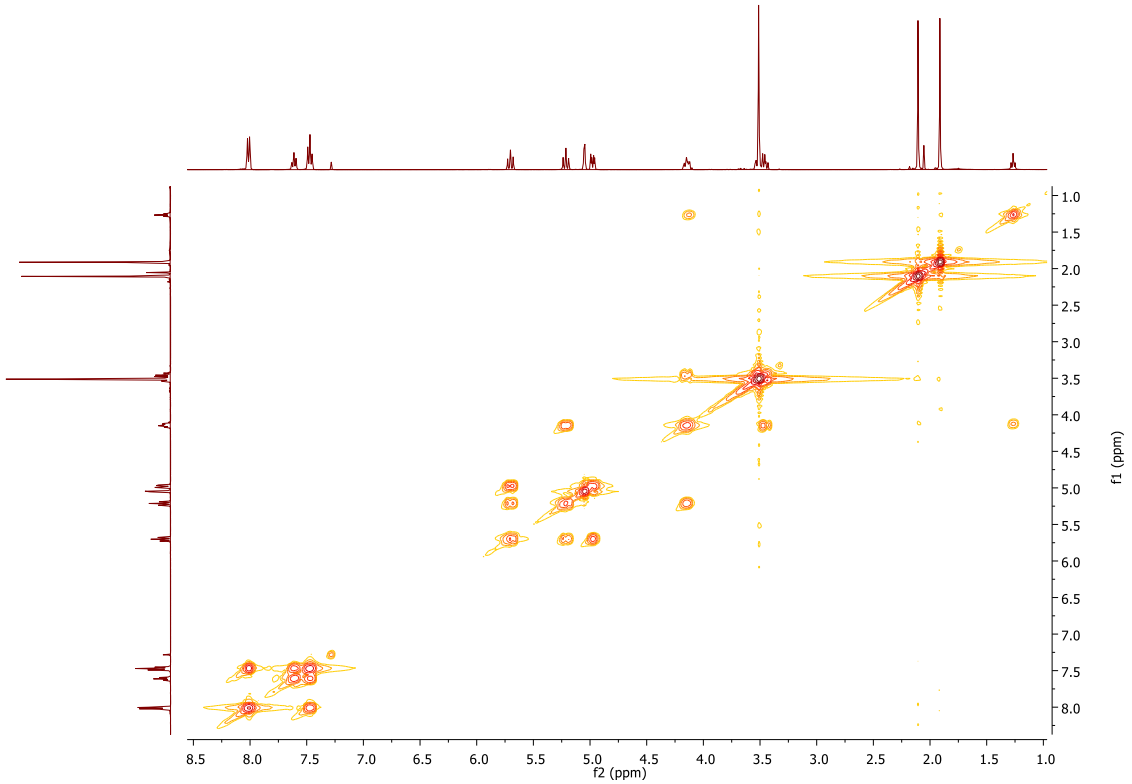

*Figure 7.19. COSY spectrum of compound **5**, in $CDCl_3$.*

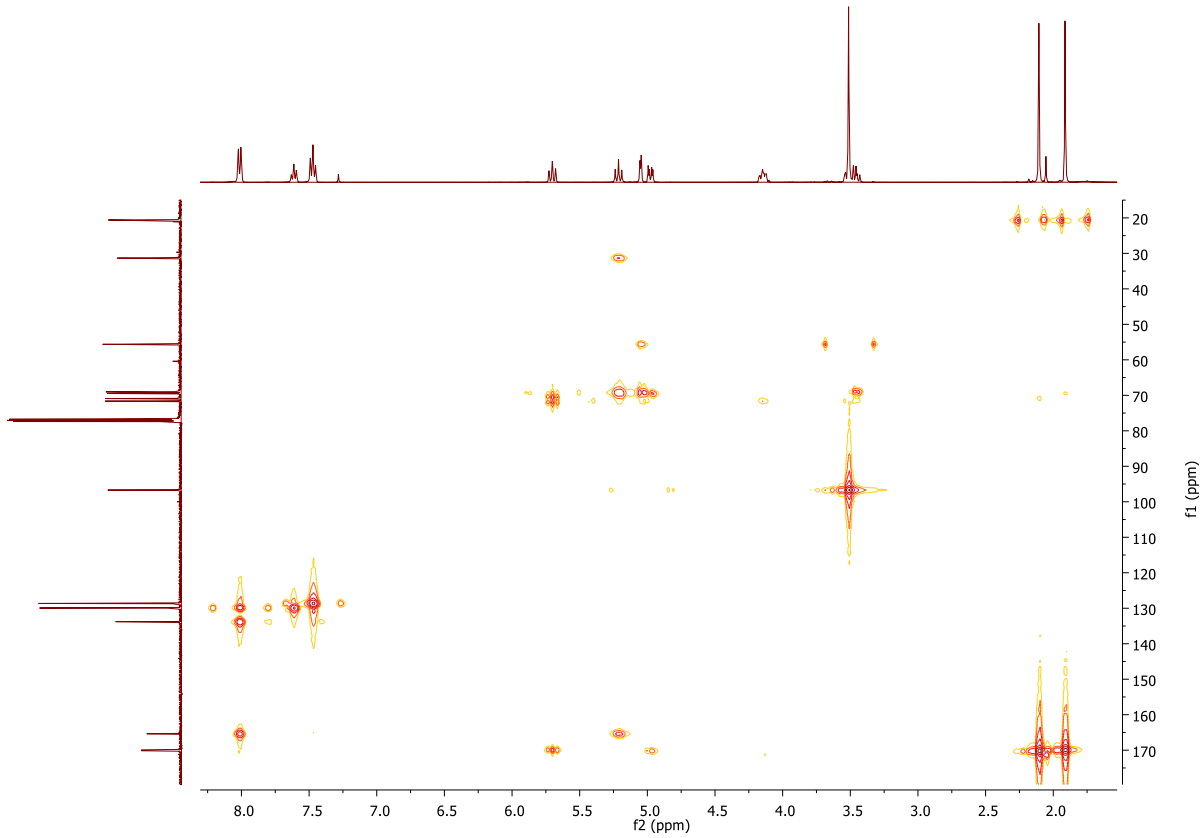

*Figure 7.20. HMBC spectrum of compound **5**, in $CDCl_3$.*

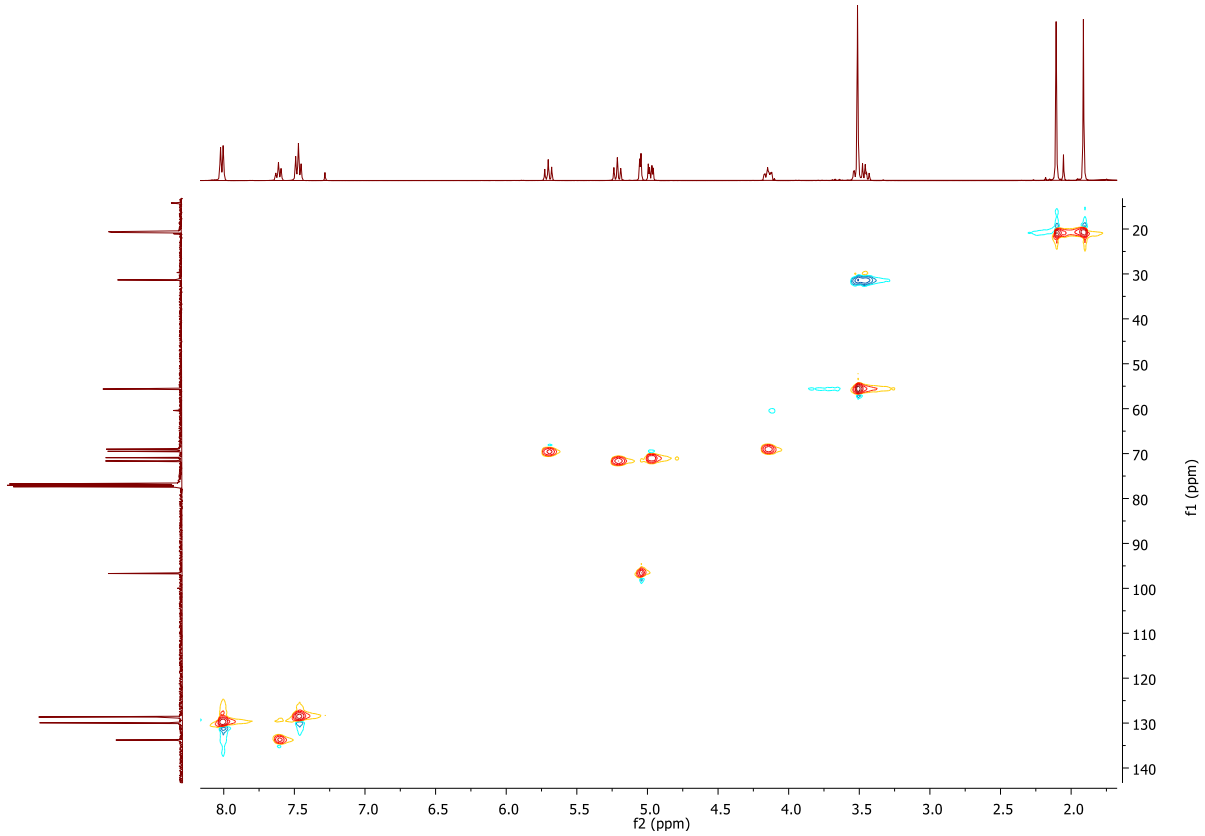

Figure 7.21. HSQC spectrum of compound **5**, *in* $CDCl_3$.